elastography is widely available, noninvasive, and shows high accuracy in staging hepatic fibrosis. However, US elastography is not carried out on patients with ascites and narrow intercostal spaces.

Gadolinium ethoxybenzyl diethylenetriaminepentaacetic acid (Gd-EOB-DTPA) is a relatively new liver-specific contrast agent on magnetic resonance imaging (MRI). Gd-EOB-DTPA is gradually taken into hepatocyte cells, resulting in signal enhancement on T1-weighted images. This contrast agent is used substantially for the detection of HCC and liver metastasis on MRI (10–13), but it also has the potential to enable functional imaging with a T1 shortening effect at the hepatobiliary phase (14–19). The measurement of the T1 relaxation time (T1RT) of liver parenchyma before and after Gd-EOB-DTPA administration allows quantitative evaluation of Gd-EOB-DTPA uptake by the liver parenchyma. T1 mapping of the liver shows the distribution of T1RT in the liver, and is useful to recognize regional or whole liver function. On the other hand, signal-based measurement on MRI is widely used for the quantification to estimate degree of liver parenchymal enhancement.

It had been reported that it was possible to assess the staging of liver fibrosis using a rat NASH model by evaluating the signal intensity-time profile after Gd-EOB-DTPA injection (15). However, the potential of using this approach to assess the staging of liver fibrosis in human has not yet been assessed. The aim of the present study was to compare four imaging approaches in liver fibrosis estimation using a quantitative parameter for the classification of fibrosis, namely, pre-enhancement T1RT, T1RT and signal-based liver-to-muscle ratio on Gd-EOB-DTPA-enhanced MRI, and liver stiffness measurement (LSM) of US elastography (FibroScan).

MATERIALS AND METHODS

Patients

The Institutional Review Board of our university hospital approved the study, and all patients received informed consent forms for approval of the MR imaging, FibroScan, and liver biopsies. The inclusion criteria were as follows: chronic HCV infection; chronic HBV infection; clinical evidence for liver cirrhosis; and NASH. The exclusion criteria were cases complicated with other liver diseases or HCC. No patients had a past history of cardiac diseases that may produce image artifact by an irregular heartbeat interval.

Both Gd-EOB-DTPA-enhanced MR examination and FibroScan were performed on 63 consecutive patients (36 men and 27 women) with chronic liver disease. Patients had a mean age of 66 years (range 37–83 years).

MRI

A clinically available 3.0 T system (Achieva; Philips Medical System, Best, Netherlands) with a 6- or 32-channel phased-array surface coil was used. The Philips Research Integrated Development Environment (PRIDE) T1 fitting tool was employed for measurement of T1RT using data from the Look-Locker echo-planar imaging sequence (T1 mapping), which was addressed previously (16). Look-Locker-Turbo-Field-Echo (LL-TFE) sequences (repetition time, 12 msec; echo time, 1.7 msec; flip angle, 7°; field of view, 420 × 285 mm; zero-fill interpolation (zip), matrix; 112 × 66 (reconstruction 256 × 256); thickness, 10 mm; acquisition time, 1 phase = 145 msec, 31 phases; and acceleration factor, 2) were obtained before and 18 minutes after 0.025 mmol/kg of Gd-EOB-DTPA (Primovist: Bayer Schering Pharma, Berlin, Germany) administration. The T1 mapping image was obtained as a single axial slice.

Our routine MR examination sequences on Gd-EOB-DTPA-enhanced MRI were T1-weighted images with in-phase and opposed-phase at pre-enhancement, 3D T1-weighted image of arterial phase, portal venous phase, respiratory-triggered T2-weighted image with fat saturation, diffusion-weighted image with low and high b factors after contrast, 3D T1-weighted image approximately 20% minutes after injection (hepatobiliary phase). The 3D T1-weighted image was obtained as T1 high-resolution isotropic volume examination (THRIVE) with fat suppression; repetition time, 3.5 msec; echo time, 1.7 msec; flip angle, 10°; field of view, 350 × 350 mm; matrix, 320 × 256; thickness, 3 mm; and reduction factor, 2). All patients received Gd-EOB-DTPA administered at 2 mL/s through an intravenous line placed in a cubital vein and flushed with 32–36 mL of 0.9% saline at the same speed. This series on Gd-EOB-DTPA-enhanced MRI was performed as a routine clinical examination to detect and characterize liver tumors.

Analysis Using Gd-EOB-DTPA-Enhanced MRI

Gd-EOB-DTPA-enhanced MRI was performed for 63 patients. In these patients, T1RT and signal-based liver to paraspinal muscle ratio (L/M ratio) were independently measured by two examiners (M.O. and M.O.) Three regions of interest (ROIs) with a range of 50–60 pixels were placed manually in the liver (liver segments of 2/3, 5, and 6/7 using Couinaud's classification), avoiding visible intrahepatic vessels on T1 mapping images and 3D T1-weighted image obtained before and 18 minutes (20 minutes) after Gd-EOB-DTPA administration. The reason why 18 minutes after Gd-EOB-DTPA administration applied is because T1RT at 18 minutes after Gd-EOB-DTPA injection has possibilities to differentiate between patients with different liver dysfunction (16). Avoiding visible intrahepatic vessels on T1 mapping images was performed in reference to 3D T1-weighted image (hepatobiliary phase) because this study was planned to measure the liver parenchymal T1 relaxation time. Mean T1RT and liver signal of the L/M ratio for the three ROIs in segments of 2/3, 5, and 6/7 were considered representative hepatic T1RT and liver signal. First, pre-enhancement T1RT was measured to analyze whether there were differences between different grades of liver fibrosis. Second, the reduction rate (RR) of the T1RT

and increasing rate (IR) of the L/M ratio of the liver parenchyma were defined as follows:

$$\text{RR of the T1RT} = [(\text{T1pre} - \text{T1post})/\text{T1pre}] \times 100\%$$

where T1pre is T1RT at pre-enhancement and T1post is T1RT at post-enhancement (18 min).

$$\text{IR of the L/M ratio} = [(\text{L/M ratio post} - \text{L/M ratio pre})/\text{L/M ratio pre}] \times 100\%$$

where L/M ratio pre is L/M ratio at pre-enhancement and L/M ratio post is L/M ratio at post-enhancement (20 min); signal of muscle was obtained for the two ROIs on the left and right paraspinal muscle and was averaged.

Analysis Using US Elastography (FibroScan)

FibroScan was performed for 63 patients by one examiner (one hepatologist with 3 years of experience in US elastography). The LSM was obtained with the right intercostal approach. The principle of elastography using FibroScan has been described elsewhere (20,21). FibroScan measured the stiffness of the liver parenchyma using both US (5 MHz) and low-frequency (50 Hz) elastic waves from an ultrasound vibrator applied to the body wall. The results expressed in kPa after 10 validated measurements were performed at a depth of 25–45 mm from the skin surface. The interquartile range (IQR) of the FibroScan was recorded to assess the reproducibility of measured results (a smaller IQR is sensitive to the FibroScan measurements).

Pathological Diagnosis and Quantification of the Liver

Fifty-eight patients received liver biopsy by one examiner (a hepatologist with 10 years of experience in liver biopsy). In all patients, the intercostal approach was used for biopsy and the biopsy was performed at liver segment 5 of Couinaud's classification. To ensure accurate histological grading of liver fibrosis using US-guided needle core biopsy, at least two samples were taken from each patient's liver using an 18G needle (MONOPTY, C.R. Bard, Murray Hill, NJ) under local anesthesia. The liver biopsy specimen was fixed in formalin and embedded in paraffin. For liver fibrosis staging, hematoxylin and eosin and Masson's trichrome stains were used.

Liver fibrosis was scored using New Inuyama Classification, which involved the use of a five-grade scale (F0–F4) (22). Experienced pathologists (two pathologists with more than 10 years of experience in liver pathology) diagnosed the stage of liver fibrosis by consensus. This system was used to grade histological lesions by means of two separate scores, one for fibrosis (F) and the other for necroinflammation (activity). The fibrosis score was defined as: F0 = no fibrosis; F1 = fibrous portal expansion; F2 = bridging fibrosis (portal-portal or portal-central linkage); F3 = bridging fibrosis with lobular distortion (disorganization); and F4 = cirrhosis.

Statistical Analysis

Data from pre-enhancement T1RT, signal-based L/M ratio, T1RT on Gd-EOB-DTPA-enhanced MRI, and LSM of FibroScan were expressed as the mean ± standard deviation (SD). In order to assess the agreement between the two observers' measurements, simple regression analysis and Bland–Altman analysis between the two measurements by two observers for pre-enhancement T1RT, RR of the T1RT, and IR of the L/M ratio in the liver parenchyma were evaluated. The strength of the correlation between the RR of the T1RT in the liver parenchyma and the LSM obtained using the FibroScan was evaluated using simple regression analysis. The diagnostic performance and the linear combination of pre-enhancement T1RT, RR of the T1RT, IR of the L/M ratio, and LSM were assessed using the receiver operating characteristic (ROC) curve, which is a plot of sensitivity versus specificity. The area under the ROC curve (AUC) and the cutoff value were obtained by ROC analysis. Statistical analyses were performed using a commercially available Excel software (Microsoft Excel 2007; Microsoft, Tokyo, Japan), StatFlex v. 6.0 software (Artech, Osaka, Japan) and free statistical software "R" (R, v. 2.6.1; The R Project for Statistical Computing; http://www.r-project.org/). $P < 0.05$ was considered statistically significant.

RESULTS

Patients

In 63 patients with Gd-EOB-DTPA-enhanced MRI and FibroScan, FibroScan had unsuccessful measurements due to ascites, obesity, and narrow intercostal space in four patients and Gd-EOB-DTPA-enhanced MRI had misregistration of liver scan in one patient. Thus, pre-enhancement T1RT, signal-based L/M ratio, RR of T1RT, and LSM of FibroScan were compared in the remaining 58 patients (34 men and 24 women) with liver biopsy (Fig. 1 shows a T1 mapping in a patient with chronic hepatitis C and F1 of New Inuyama Classification). Chronic liver diseases were nonalcoholic fatty liver disease (NAFLD; $n = 25$), chronic hepatitis C ($n = 15$), chronic hepatitis B ($n = 4$), NASH ($n = 3$), alcoholic liver disease ($n = 2$), and liver cirrhosis ($n = 9$). There were Grade A ($n = 42$), Grade B ($n = 15$), and Grade C ($n = 1$) by Child-Pugh Classification in 58 patients.

The distribution of these scores for fibrosis were as follows: F0, $n = 13$; F1, $n = 14$; F2, $n = 12$; F3, $n = 10$; and F4, $n = 9$.

Agreement Between the Two observers' Measurements

Simple regression analysis and Bland–Altman analysis showed narrow limits of agreement between two observers' measurements of pre-enhancement T1RT,

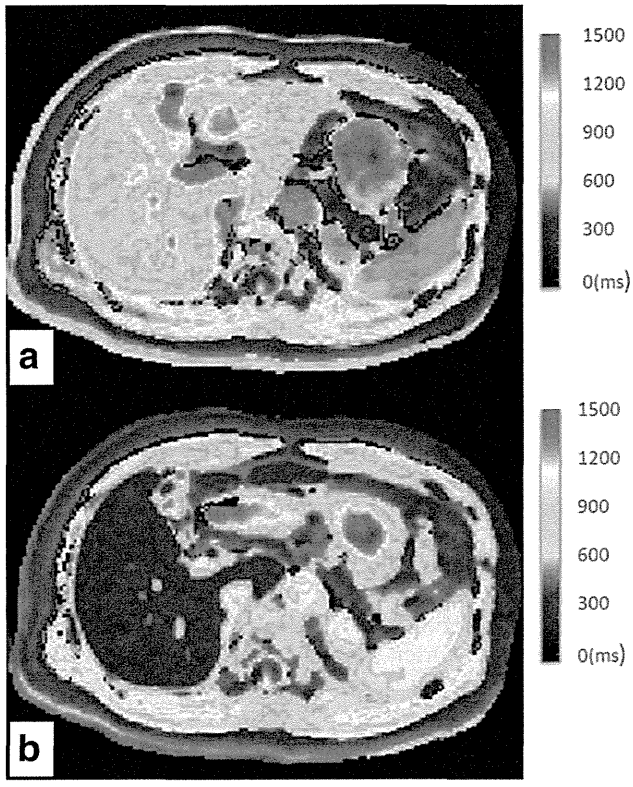

Figure 1. T1 mapping of a 64-year-old man (New Inuyama Classification: F1) with chronic HCV infection on Gd-EOB-DTPA-enhanced MRI. **a:** Pre-enhancement T1 mapping. Number in the right upper corner shows the scale of T1 relaxation time (T1RT). Mean T1RT for the three ROIs in segments of 2/3, 5, and 6/7 is considered representative T1RT for the liver. Pre-enhancement mean T1RT was 782.0 msec. **b:** Post-enhancement T1 mapping at 18 minutes. Number in the right upper corner shows the scale of T1RT. Mean T1RT for the three ROIs is considered representative T1RT for the liver. Mean T1RT at 18 minutes after enhancement was 256.2 msec. Thus, the reduction rate (RR = [(T1pre – T1post) / T1pre] × 100%) of the T1RT of liver parenchyma is 67.2%.

RR of the T1RT, and IR of the L/M ratio (Fig. 2). Bland–Altman analysis yielded narrow limits of agreement for pre-enhancement T1RT, RR of the T1RT, and IR of the L/M ratio.

T1 Relaxation Time Measurement

The average length of time between the date of Gd-EOB-DTPA-enhanced MRI and that of liver biopsy was 68 days (range 0–156 days). The mean ± SD of pre-enhancement T1RT was 822 ± 93 msec (range; 685–1037 msec). The mean ± SD of RR of T1RT was 53.8 ± 10.2% (range; 34.5–68.7%). The distribution (box-and-whisker plots) of the pre-enhancement T1RT and the RR of the T1RT are shown in Figs. 3 and 4. The mean ± SD of pre-enhancement T1RT increased with the degree of fibrosis (F0-F1, 825 ± 90.1 msec, versus F2-F3-F4, 850 ± 94.1 msec, $P = 0.075$, F0-F1-F2, 819 ± 83.8 msec versus F3-F4, 875 ± 98.6 msec, $P = 0.41$ and F0-F1, 825 ± 90.1 msec versus F2-F3, 829 ± 92.7 msec, $P = 0.96$.

The mean ± SD of RR determined using T1RT decreased with the degree of fibrosis (F0-F1, 58.5 ± 6.2%, versus F2-F3-F4, 48.8 ± 11.7%, $P = 0.010$, F0-F1-F2, 58.2 ± 6.2% versus F3-F4, 45.5 ± 12.3%, $P = 0.010$ and F0-F1, 58.5 ± 6.2% versus F2-F3, 52.1 ± 12.0%, $P = 0.0038$).

Thus, the RR of T1RT showed significant differences to differentiate F0-F1 from F2-F3-F4, F0-F1-F2 from F3-F4, F0-F1 from F2-F3, although the pre-enhancement T1RT did not show significant differences.

Signal-Based Liver-to-Muscle Ratio

The mean ± SD of IR of L/M ratio was 59.7 ± 19.4% (range; 24.2–83.2%). The mean ± SD of IR of L/M ratio decreased with the degree of fibrosis (F0-F1, 61.5 ± 19.6%, versus F2-F3-F4, 55.2 ± 11.8%, $P = 0.47$, F0-F1-F2, 59.8 ± 17.2% versus F3-F4, 54.9 ± 13.3%, $P = 0.21$ and F0-F1, 61.5 ± 19.6% versus F2-F3, 55.5 ± 7.3%, $P = 0.52$). Thus, the IR of L/M ratio did not show significant differences to differentiate F0-F1 from F2-F3-F4, F0-F1-F2 from F3-F4, F0-F1 from F2-F3.

The distribution (box-and-whisker plots) of the IR of L/M ratio is shown in Fig. 5.

LSM of US Elastography

The average length of time between the dates of the FibroScan and the liver biopsy was 53 days (range 0–143 days). The mean ± SD of LSM obtained using the FibroScan was 12.4 ± 15.8 kPa (range; 2.7–55.0 kPa). The mean ± SD of IQR on the FibroScan was 2.3 ± 3.3 kPa (range; 0–11.9 kPa) for all patients. The distribution (box-and-whisker plots) of the LSM is shown in Fig. 6.

The LSM increased in line with the degree of fibrosis (F0-F1, 5.4 ± 2.2 kPa versus F2-F3-F3, 19.3 ± 15.5 kPa, $P = 0.0011$, F0-F1-F2, 6.8 ± 3.6 kPa versus F3-F4, 23.8 ± 17.1 kPa, $P = 0.0029$, and F0-F1, 5.4 ± 2.2 kPa versus F2-F3, 11.4 ± 7.2 kPa, $P = 0.0098$).

Thus, the LSM of FibroScan showed significant differences to differentiate F0-F1 from F2-F3-F4, F0-F1-F2 from F3-F4, F0-F1 from F2-F3.

Correlation Between T1 Mapping, Signal-Based Liver-to-Muscle Ratio, and FibroScan

The average length of time between the date of Gd-EOB-DTPA-enhanced MRI and FibroScan was 16 days (range, 0–27 days). Figure 7 shows a correlation diagram regarding the Gd-EOB-DTPA-enhanced MRI and FibroScan. In comparing the levels of LSM obtained using FibroScan with the RR of T1RT, a negative correlation was found ($r = -0.65$, $P = 0.00005$).

In discriminating between patients with F3-F4 liver fibrosis, the AUCs from the ROC analysis were 0.83 (cutoff value 53.5%. sensitivity 0.80, specificity 0.71) for the RR of T1RT and 0.83 for the LSM (cutoff value 13.8 kPa, sensitivity 0.73, specificity 0.90) (Fig. 8a, Table 1). The AUCs from the ROC analysis in patients with F2-F3-F4 fibrosis on histology were 0.72 (cutoff value 56.8%, sensitivity 0.71, specificity 0.64) for the RR of T1RT and 0.88 (cutoff value 9.6 kPa, sensitivity 0.76, specificity 0.92) for the LSM (Fig. 8b, Table 1). In discriminating between patients with F2-F3 liver

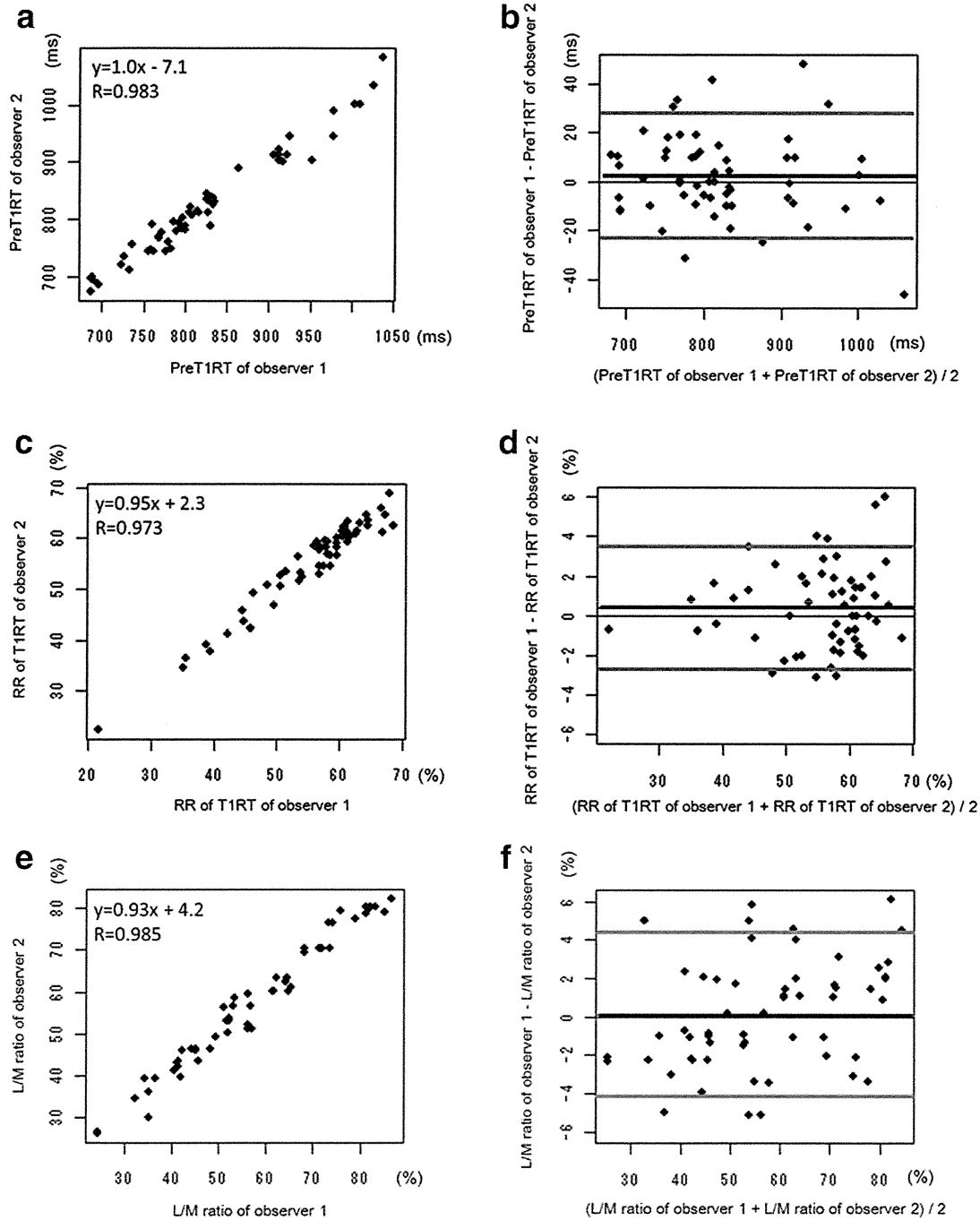

Figure 2. Agreement between the two observers' measurements. Simple regression analyses (**a**: pre-enhancement T1RT, **c**: RR of the T1RT, **e**: IR of the L/M ratio) and Bland–Altman analyses of agreement (**b**: pre-enhancement T1RT, **d**: RR of the T1RT, **f**: IR of the L/M ratio) between the two measurements are displayed. Simple regression analysis showed a high correlation between the means of the observers' manual measurements of pre-enhancement T1RT, RR of the T1RT, IR of the L/M ratio in the liver parenchyma. Bland–Altman analysis yielded narrow limits of agreement of −23 to 28 msec for pre-enhancement T1RT, of −2.7 to 3.5% for RR of the T1RT, and of −4.1 to 4.4% for the L/M ratio. Black line (center) = mean of differences. Gray lines (top and bottom) = upper and lower limits of agreement (mean difference, ±2 SD). pre T1RT; precontrast T1 relaxation time, RR of T1RT; reduction rate of T1 relaxation time, L/M ratio; liver to paraspinal muscle ratio.

fibrosis, the AUCs from the ROC analysis were 0.68 (cutoff value 59.4%. sensitivity 0.64, specificity 0.72) for the RR of T1RT and 0.81 for the LSM (cutoff value 5.5 kPa, sensitivity 0.81, specificity 0.71) (Fig. 8c, Table 1).

The capability of LSM was better than that of RR of T1RT, pre-enhancement T1RT, and L/M ratio to differentiate $F \geq 2$, but LSM and RR of T1RT showed the same value to differentiate $F \geq 3$ (Fig. 8a–c, Table 1).

DISCUSSION

We assessed the efficacy of T1RT on Gd-EOB-DTPA-enhanced MRI (T1 mapping) for the evaluation of the

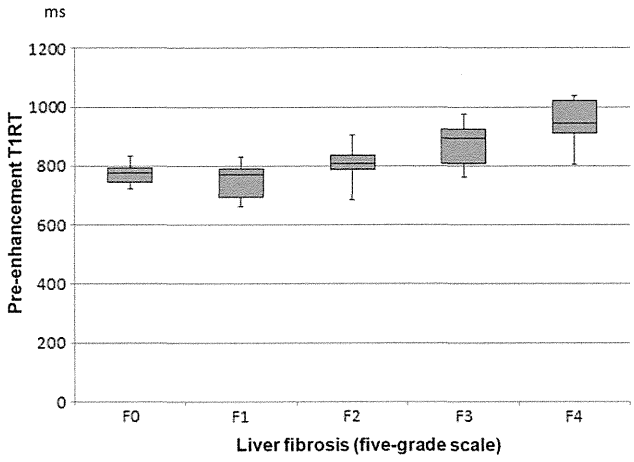

Figure 3. Box-and-whisker plots of pre-enhancement T1 relaxation time. The distribution of pre-enhancement T1RT is shown for New Inuyama Classification fibrosis stages (F0–F4) in patients who had liver biopsy. F0 = no fibrosis; F1 = fibrous portal expansion; F2 = bridging fibrosis (portal-portal or portal-central linkage); F3 = bridging fibrosis with lobular distortion (disorganization); and F4 = cirrhosis.

severity of liver fibrosis, in patients with chronic liver diseases. In our study, we found that the RR of T1RT measured before and 18 minutes after Gd-EOB-DTPA injection was inversely correlated with the LSM index determined by FibroScan. Both the RR of T1RT and the LSM measurement using FibroScan performed well (AUC: RR = 0.83 and LSM = 0.83) in the diagnosis of patients with fibrosis of grade $F \geq 3$. However, the use of RR of T1RT (AUC: 0.72) for the diagnosis of patients with fibrosis of grade $F \geq 2$ seemed to be somewhat less sensitive than the LSM (AUC: 0.88),

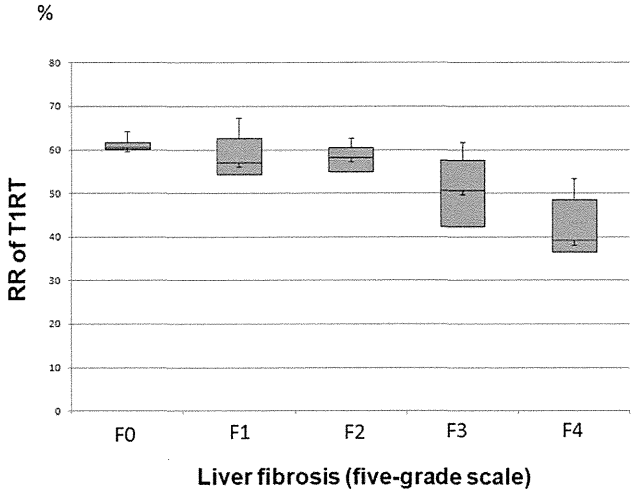

Figure 4. Box-and-whisker plots of reduction rate of T1 relaxation time on Gd-EOB-DTPA-enhanced MRI. The distribution of RR of T1RT on Gd-EOB-DTPA-enhanced MRI is shown for fibrosis stages (F0–F4) in patients who had liver biopsy. RR of T1RT of the liver parenchyma is defined as follows; RR = [(T1pre – T1post) / T1pre] × 100 (%), where T1pre is T1RT at pre-enhancement and T1post is T1RT at post-enhancement (18 min). F0 = no fibrosis; F1 = fibrous portal expansion; F2 = bridging fibrosis (portal-portal or portal-central linkage); F3 = bridging fibrosis with lobular distortion (disorganization); and F4 = cirrhosis.

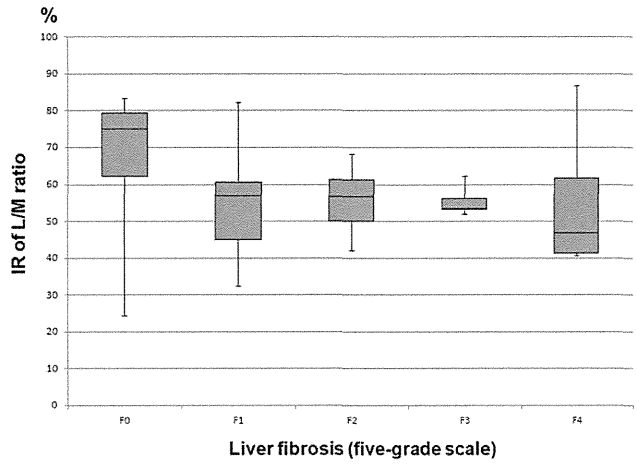

Figure 5. Box-and-whisker plots of increasing rate of liver to paraspinal muscle ratio on Gd-EOB-DTPA-enhanced MRI. The distribution of increasing rate (IR) of signal-based liver to paraspinal muscle ratio (L/M ratio) on Gd-EOB-DTPA-enhanced MRI is shown for fibrosis stages (F0–F4) in patients who had liver biopsy. IR of L/M ratio of the liver parenchyma is defined as follows; IR of the L/M ratio = [(L/M ratio post- – L/M ratio pre) / L/M ratio pre] × 100%, where L/M ratio pre is L/M ratio at pre-enhancement and L/M ratio post is L/M ratio at post-enhancement (20 min). F0 = no fibrosis; F1 = fibrous portal expansion; F2 = bridging fibrosis (portal-portal or portal-central linkage); F3 = bridging fibrosis with lobular distortion (disorganization); and F4 = cirrhosis.

because a certain degree of overlap among lower stages of liver fibrosis existed. Therefore, the RR of T1RT and the LSM of FibroScan were not equivalent, especially in patients with mild fibrosis. But T1RT by noninvasive means may be available for the diagnosis of relatively severe liver cirrhosis (fibrosis of grade $F \geq 3$), and be used as an alternative to FibroScan. In our study, the RR of T1RT and LSM of FibroScan showed significant differences to differentiate $F \geq 2$

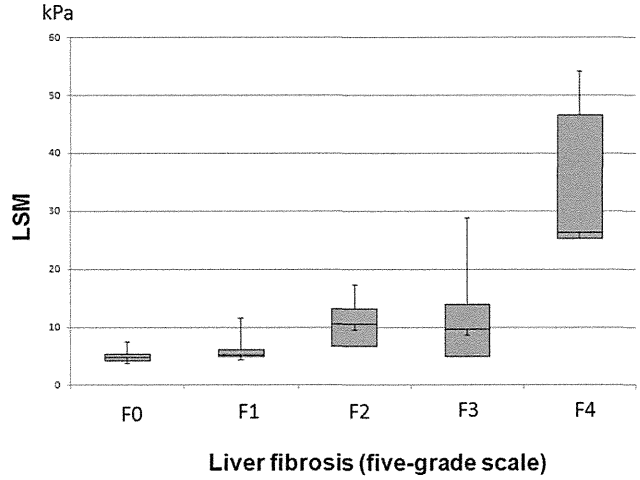

Figure 6. Box-and-whisker plots of liver stiffness measurement on FibroScan. The distribution of LSM of FibroScan in patients who had liver biopsy. Box-and-whisker plots of LSM on FibroScan is shown for fibrosis stages (F0–F4) in patients who had liver biopsy. F0 = no fibrosis; F1 = fibrous portal expansion; F2 = bridging fibrosis (portal-portal or portal-central linkage); F3 = bridging fibrosis with lobular distortion (disorganization); and F4 = cirrhosis.

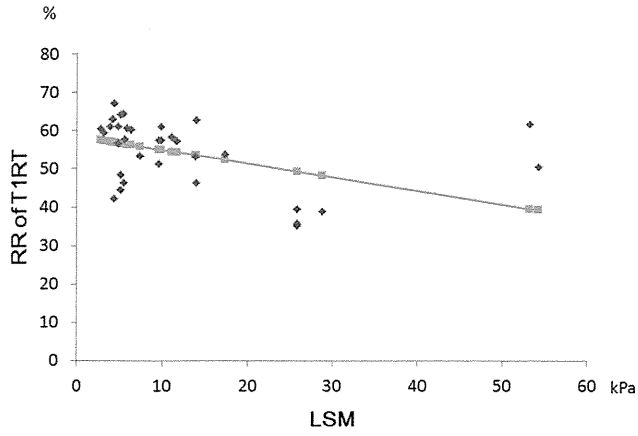

Figure 7. Correlation diagram between LSM of FibroScan and reduction rate of T1RT on Gd-EOB-DTPA-enhanced MRI. Spearman rank correlation was used to investigate the relation between LSM and RR of T1RT. There is a negative correlation between LSM and RR ($r = -0.65$, $P = 0.00005$).

and $F \geq 3$, although the pre-enhancement T1RT and IR of L/M ratio did not show significant differences. Thus, the RR of T1RT is helpful for staging of liver cirrhosis, especially in patients with $F \geq 3$.

Liver fibrosis occurs due to a scarring process and deposition of collagen and causes hepatic dysfunction. However, the relationship between hepatocyte function and fibrosis is not well understood. To facilitate a more quantitative evaluation of liver cirrhosis on Gd-EOB-DTPA-enhanced MRI, we focused on T1RT. This was due to the fact that changes in the T1 relaxation rate were considered directly proportional to the amount of contrast agent taken up by hepatocyte cells (23). On the other hand, changes in the signals of T1-weighted images after the injection of Gd-related contrast agent, such as Gd-EOB-DTPA, were not considered directly proportional to the concentration of contrast agent (24) because MR signal intensity does not show a linear relationship with the Gd-EOB-DTPA concentration. In recent reports, liver function studies using signal enhancement with Gd-EOB-DTPA (25,26) have been analyzed using ROI-based measurements; for example, the signal from the liver was subtracted between the phases or normalized with that in other organs. However, in these measurements there was a risk that signal enhancement could lose objectivity because the pixel value could be easily affected by extrinsic factors such as receiver gain and tuning MRI radiofrequency coils. Therefore, we believed that T1RT is a better method to evaluate the uptake of Gd-EOB-DTPA to the liver.

When liver MRI is performed for the purpose of detection and characterization of liver tumors, we suggest that T1 mapping could be used as an adjunct to routine imaging, to assess the degree of liver fibrosis in patients with liver diseases. Liver fibrosis can occur either homogeneously or heterogeneously. Therefore, we suggest that the grading of fibrosis should be estimated using T1 mapping in each liver segment, using a classification system such as that developed by Couinaud. Our method using T1RT measurement provides an evaluation of parenchymal changes in different liver segments, enabling accurate evaluation of disease severity in cases in which the fibrosis is not uniform across the entire liver.

Gd-EOB-DTPA-enhanced MRI allows the assessment of not only liver cirrhosis, but also hepatic tumors. In particular, this modality has the potential for early detection of HCC (12,13). FibroScan has a disadvantage of no combination with grayscale sonography for screening of liver tumors, because FibroScan is a dedicated device for the evaluation for liver stiffness. The development of a noninvasive method for the assessment of liver fibrosis involving T1RT represents a major advance in the management of chronic liver diseases. As several authors have stated, evaluation of the kinetic distribution of Gd-EOB-DTPA during the hepatobiliary phase is a promising method for understanding hepatocyte function (14–16,27). The difference in contrast between liver tumors and the parenchyma is affected by liver function, which is mediated by hepatocyte cells.

Noninvasive imaging of liver fibrosis, involving modalities such as US, computed tomography (CT), and MRI, is currently used in patients with chronic liver disease and suspected HCC. In particular, US elastography (7,8) and MR elastography (28,29) are receiving increasing attention. US elastography has been recognized as the easiest device for noninvasive imaging. FibroScan is considered a reliable method for the diagnosis of severe fibrosis and cirrhosis (30), but a certain degree of overlap among lower stages of liver fibrosis has been reported (31). Limitations associated with the FibroScan should be mentioned and include its use regarding obese patients, patients with a narrow intercostal space, and patients with ascites, liver atrophy, space occupying lesions in the liver (32), and the exclusion of the left lobe due to heartbeat and depth location of imaging. In addition, one-dimensional (1D) US imaging with the propagation speed of a wave, using pulse-echo US for FibroScan, is different from two-dimensional (2D) MRI such as T1 mapping with Gd-EOB-DTPA. Another promising method is MR elastography. This modality quantifies the viscoelastic parameters of the liver by measuring acoustic shear waves through the liver tissue (28). Several reports support the observation that a normal mean liver stiffness value obtained using MR elastography in the setting of chronic liver disease is consistent with a liver fibrosis score of F0 on pathology (28), while other fibrosis scores (F1–F4) are also diagnosed accurately (28,33). This method does not require MR contrast agents and may be more cost-effective than T1RT with Gd-EOB-DTPA, although additional equipment is required for MR elastography.

Diffusion-weighted imaging (DWI) of the liver is also useful for assessing liver fibrosis. Decreased apparent diffusion coefficient (ADC) is caused by the decrease in total hepatic blood flow in cirrhosis. Intravoxel incoherent motion (IVIM) analysis is based on a method that enables separate determination of coefficients with molecular diffusion of water and microcirculation of blood in the capillary network in each imaging voxel. IVIM may serve as a valuable tool for assessing liver fibrosis, because it reflects decreased capillary

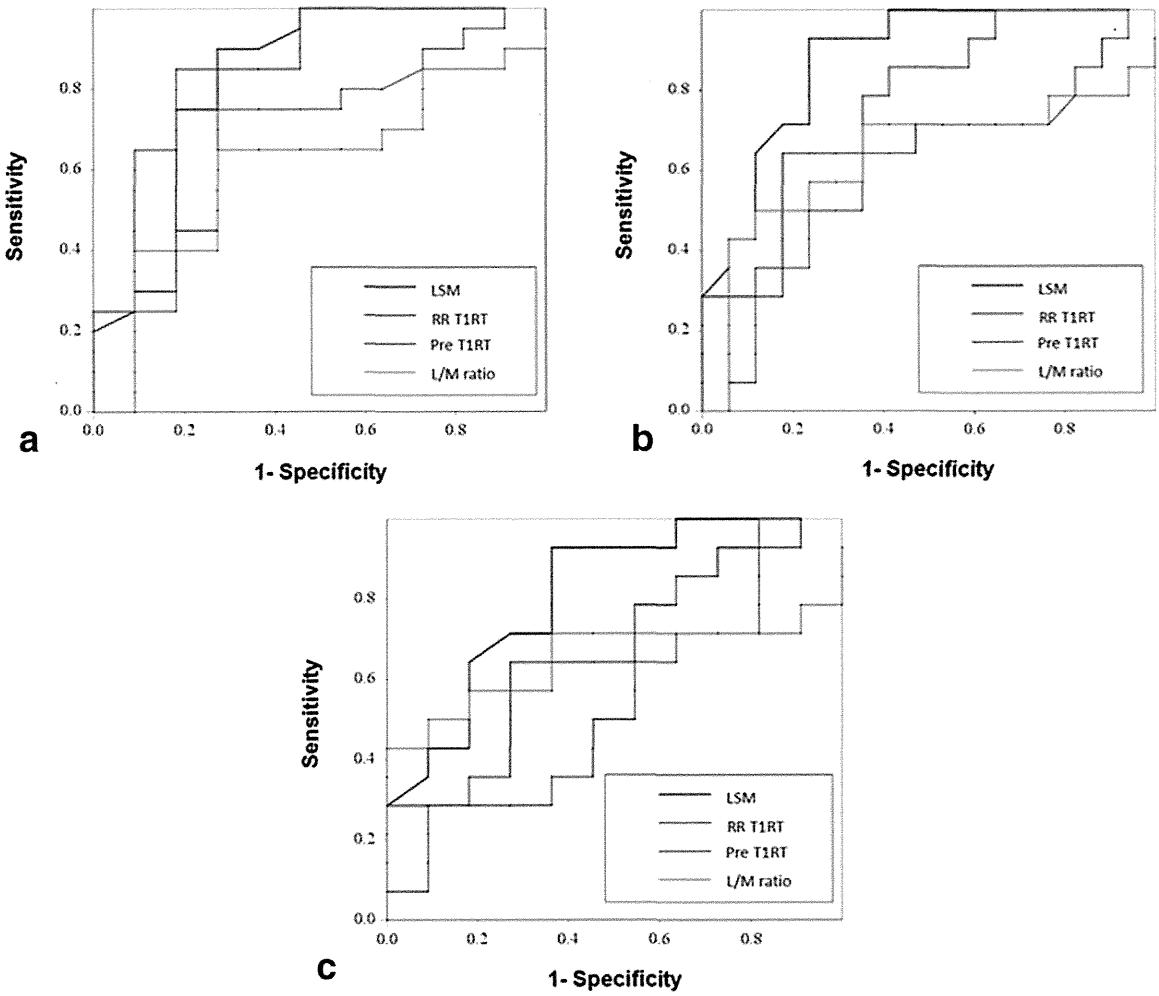

Figure 8. ROC curves of RR of T1RT, LSM, pre T1RT, and liver to paraspinal muscle ratio (L/M ratio) for F3-F4 fibrosis stages. On the ROC curves of RR of T1RT, LSM, pre-enhancement T1RT, and liver to paraspinal muscle ratio (L/M ratio), area under the receiving operating curve (AUC), cutoff value between F3-F4 and F0-F1-F2, sensitivity and specificity are shown in the Table 1. **a:** ROC curves of LSM (AUC, 0.83) and RR of T1RT (AUC, 0.83) were superior to pre-enhancement T1RT (AUC, 0.67) and L/M ratio (AUC, 0.61). **b:** ROC curves of RR of T1RT, LSM, pre-enhancement T1RT and L/M ratio for F2-F3-F4 fibrosis stages. On ROC curves of RR of T1RT, LSM, pre-enhancement T1RT, and L/M ratio, LSM (AUC, 088) was superior to RR of T1RT (AUC, 0.72), pre-enhancement T1RT (AUC, 0.59) and L/M ratio (AUC, 0.63). Cutoff value, sensitivity, and specificity are shown in Table 1. **c:** ROC curves of RR of T1RT, LSM, pre-enhancement T1RT and L/M ratio for F2-F3 fibrosis stages. On ROC curves of RR of T1RT, LSM, pre-enhancement T1RT, and L/M ratio, LSM (AUC, 081) was superior to RR of T1RT (AUC, 0.68), pre-enhancement T1RT (AUC, 0.50), and L/M ratio (AUC, 0.65). Cutoff value, sensitivity, and specificity are shown in Table 1.

perfusion as well as alterations in pure molecular water diffusion in cirrhotic livers (34). But technical factors, such as cardiac motion limiting evaluation of the left hepatic lobe and respiratory motion effecting ADC values in the right hepatic lobe, need to be addressed with respiratory-triggered techniques.

Perfusion-weighted imaging (PWI) of the liver is employed by dual-input one-compartment analysis and has permitted measurement of flow parameters such as hepatic arterial/portal venous inflow rate, absolute hepatic arterial/portal venous blood flow, hepatic arterial/portal venous fraction, mean transit time, and distribution volume. PWI is correlated with the severity of cirrhosis and portal hypertension (35). But PWI cannot directly reflect the fibrosis component alone, because the analysis is substantially based on vascular flow and perfusion.

The present study had some limitations. First, T1 mapping may not provide the T1RT at exactly the same location in the liver as the FibroScan and liver biopsy, due to the fact that the T1 mapping image in our study was obtained as a single axial slice. Second, our analysis using T1 mapping could not always reflect the fibrosis component alone. There was a lack of analysis of other factors that might influence elasticity, such as steatosis, iron overload, vascular flow, and perfusion (36). In addition, the relationship between fibrosis (F-factor) and necroinflammation (activity) on histological examination was not investigated in our study. Further analysis is required. Third, the uptake of Gd-EOB-DTPA in the hepatocyte allows shortening T1RT, which links to the Gd-EOB-DTPA concentration at the hepatobiliary phase. The contrast agent enters the hepatocytes through the

Table 1
Receiver Operating Characteristic (ROC) Analysis

	LSM	RR of T1RT	Pre T1RT	L/M ratio
F012–34				
AUC	0.83	0.83	0.67	0.61
Cutoff	13.8	53.5	863	56.7
Sens.	0.73	0.80	0.72	0.65
Spec.	0.90	0.71	0.75	0.73
F01–234				
AUC	0.88	0.72	0.59	0.63
Cutoff	9.60	56.8	831	56.7
Sens.	0.76	0.71	0.64	0.71
Spec.	0.92	0.64	0.64	0.64
F01–23				
AUC	0.81	0.68	0.50	0.65
Cutoff	5.50	59.4	831	56.7
Sens.	0.81	0.64	0.54	0.71
Spec.	0.71	0.72	0.64	0.63

LSM, liver stiffness measurement (unit, kPa); RR of T1RT, reduction rate of T1 relaxation time (unit, %); pre T1RT; precontrast T1 relaxation time (unit, msec); L/M ratio, liver to paraspinal muscle ratio on signal based measurement (unit, %); F012–34, fibrosis grade of New Inuyama Classification; F012 versus F34, F01–234, F01 versus F234, F01–23; F01 versus F23; AUC, area under the ROC curve; Sens., sensitivity; Spec., specificity.

organic anion transporting polypeptides (OATP) 1B1 (OATP1B1) and/or OATP1B3, and it is excreted into the bile via multidrug resistance protein 2 (MRP2) (37). But the parameter of T1RT cannot distinguish the excretion from the uptake of Gd-EOB-DTPA, because the concentration of these transporters in patients with liver fibrosis is unknown. Therefore, we should know the expression rate of OATP1B1, OATP1B3, and MRP2 in grading of liver cirrhosis. Further elucidation to assess the correlation between the expression of sinusoidal and canalicular transporters and T1RT of Gd-EOB-DTPA-enhanced MRI is needed.

Fourth, biopsy specimens that do not meet the scoring criteria of the New Inuyama Classification are associated with a high risk of understaging (38). In addition, further investigation is required as to whether or not there are differences between specimen biopsies and images (T1 mapping and FibroScan). Fifth, the effects of cardiac function were not investigated at FibroScan examination, although patients had no past history of cardiac diseases (cardiac function may be a potentially influential factor in the use of FibroScan) (39). Sixth, the maximum length of time between the date of Gd-EOB-DTPA-enhanced MRI (or FibroScan) and that of liver biopsy was 156 (or 143) days. In these patients, the amount of fibrosis may change. However, we believe there may be no apparent change of liver fibrosis in these patients, because the progression rate of liver fibrosis is known as 0.1 unit/year (for example, it takes ~10 years from F1 to F2) (40).

In conclusion, the estimation of the RR determined using T1RT of T1 mapping with Gd-EOB-DTPA is a noninvasive tool for assessing liver fibrosis, and it is inversely correlated with the LSM obtained using FibroScan. Our result proved the noninferiority of T1 mapping for noninvasive diagnosis of liver fibrosis in comparison with US elastography, especially in patients with severe fibrosis, such as F3-F4, because the diagnostic accuracy of T1 mapping is almost the same as that of US elastography. But these interpretations remain speculative due to the limited number of patients enrolled in our study. Further studies are recommended to confirm the superiority of T1 mapping in the assessment of liver fibrosis because this new technique has not yet been validated in large clinical trials.

REFERENCES

1. Schiff ER, Lee SS, Chao YC, et al. Long-term treatment with entecavir induces reversal of advanced fibrosis or cirrhosis in patients with chronic hepatitis B. Clin Gastroenterol Hepatol 2011;9:274–276.
2. Chang TT, Liaw YF, Wu SS, et al. Long-term entecavir therapy results in the reversal of fibrosis/cirrhosis and continued histological improvement in patients with chronic hepatitis B. Hepatology 2010;52:886–893.
3. Poynard T, Bedossa P, Opolon P. Natural history of liver fibrosis progression in patients with chronic hepatitis C. The OBSVIRC, METAVIR, CLINIVIR, and DOSVIRC groups. Lancet 1997;349:825–832.
4. Parkes J, Guha IN, Roderick P, Rosenberg W. Performance of serum marker panels for liver fibrosis in chronic hepatitis C. J Hepatol 2006;44:462–474.
5. Bravo AA, Sheth SG, Chopra S. Liver biopsy. N Engl J Med 2001;344:495–500.
6. Piccinino F, Sagnelli E, Pasquale G, Giusti G. Complications following percutaneous liver biopsy. A multicentre retrospective study on 68,276 biopsies. J Hepatol 1986;2:165–173.
7. Koizumi Y, Hirooka M, Kisaka Y, et al. Liver fibrosis in patients with chronic hepatitis C: noninvasive diagnosis by means of real-time tissue elastography—establishment of the method for measurement. Radiology 2011;258:610–617.
8. Tatsumi C, Kudo M, Ueshima K, et al. Noninvasive evaluation of hepatic fibrosis using serum fibrotic markers, transient elastography (FibroScan) and real-time tissue elastography. Intervirology 2008;51(Suppl 1):27–33.
9. Ziol M, Handra-Luca A, Kettaneh A, et al. Noninvasive assessment of liver fibrosis by measurement of stiffness in patients with chronic hepatitis C. Hepatology 2005;41:48–54.
10. Ichikawa T, Saito K, Yoshioka N, et al. Detection and characterization of focal liver lesions: a Japanese phase III, multicenter comparison between gadoxetic acid disodium-enhanced magnetic resonance imaging and contrast-enhanced computed tomography predominantly in patients with hepatocellular carcinoma and chronic liver disease. Invest Radiol 2010;45:133–141.
11. Zech CJ, Herrmann KA, Reiser MF, Schoenberg SO. MR imaging in patients with suspected liver metastases: value of liver-specific contrast agent Gd-EOB-DTPA. Magn Reson Med Sci 2007;6:43–52.
12. Kogita S, Imai Y, Okada M, et al. Gd-EOB-DTPA-enhanced magnetic resonance images of hepatocellular carcinoma: correlation with histological grading and portal blood flow. Eur Radiol 2010;20:2405–2413.
13. Okada M, Imai Y, Kim T, et al. Comparison of enhancement patterns of histologically confirmed hepatocellular carcinoma between gadoxetate- and ferucarbotran-enhanced magnetic resonance imaging. J Magn Reson Imaging 2010;32:903–913.
14. Tsuda N, Okada M, Murakami T. Potential of gadolinium-ethoxybenzyl-diethylenetriamine pentaacetic acid (Gd-EOB-DTPA) for differential diagnosis of nonalcoholic steatohepatitis and fatty liver in rats using magnetic resonance imaging. Invest Radiol 2007;42:242–247.
15. Tsuda N, Okada M, Murakami T. New proposal for the staging of nonalcoholic steatohepatitis: evaluation of liver fibrosis on Gd-EOB-DTPA-enhanced MRI. Eur J Radiol 2010;73:137–142.
16. Katsube T, Okada M, Kumano S, et al. Estimation of liver function using T1 mapping on Gd-EOB-DTPA-enhanced magnetic resonance imaging. Invest Radiol 2011;46:277–283.

17. Goshima S, Kanematsu M, Watanabe H, et al. Gd-EOB-DTPA-enhanced MR imaging: prediction of hepatic fibrosis stages using liver contrast enhancement index and liver-to-spleen volumetric ratio. J Magn Reson Imaging 2012;36:1148–1153.
18. Nishie A, Asayama Y, Ishigami K, et al. MR prediction of liver fibrosis using a liver-specific contrast agent: superparamagnetic iron oxide versus Gd-EOB-DTPA. J Magn Reson Imaging 2012; 36:664–671.
19. Norén B, Forsgren MF, Dahlqvist Leinhard O, et al. Separation of advanced from mild hepatic fibrosis by quantification of the hepatobiliary uptake of Gd-EOB-DTPA. Eur Radiol 2013;23:174–181.
20. Sandrin L, Fourquet B, Hasquenoph JM, et al. Transient elastography: a new noninvasive method for assessment of hepatic fibrosis. Ultrasound Med Biol 2003;29:1705–1713.
21. Sandrin L, Tanter M, Gennisson JL, Catheline S, Fink M. Shear elasticity probe for soft tissues with 1-D transient elastography. IEEE Trans Ultrason Ferroelectr Freq Control 2002;49:436–446.
22. Ichida F, Tsuji T, Omata M et al. New Inuyama classification; new criteria for histological assessment of chronic hepatitis. Int Hepatol Commun 1996;6:112–119.
23. Rosen BR, Belliveau JW, Vevea JM, Brady TJ. Perfusion imaging with NMR contrast agents. Magn Reson Med 1990;14:249–265.
24. Stanisz GJ, Henkelman RM. Gd-DTPA relaxivity depends on macromolecular content. Magn Reson Med 2000;44:665–667.
25. Tamada T, Ito K, Higaki A, et al. Gd-EOB-DTPA-enhanced MR imaging: evaluation of hepatic enhancement effects in normal and cirrhotic livers. Eur J Radiol 2011;80:e311–316.
26. Motosugi U, Ichikawa T, Sou H, et al. Liver parenchymal enhancement of hepatocyte-phase images in Gd-EOB-DTPA-enhanced MR imaging: which biological markers of the liver function affect the enhancement? J Magn Reson Imaging 2009;30: 1042–1046.
27. Hamm B, Staks T, Muhler A, et al. Phase I clinical evaluation of Gd-EOB-DTPA as a hepatobiliary MR contrast agent: safety, pharmacokinetics, and MR imaging. Radiology 1995;195:785–792.
28. Rouviere O, Yin M, Dresner MA, et al. MR elastography of the liver: preliminary results. Radiology 2006;240:440–448.
29. Salameh N, Larrat B, Abarca-Quinones J, et al. Early detection of steatohepatitis in fatty rat liver by using MR elastography. Radiology 2009;253:90–97.
30. Boursier J, de Ledinghen V, Zarski JP, et al. A new combination of blood test and FibroScan for accurate non-invasive diagnosis of liver fibrosis stages in chronic hepatitis C. Am J Gastroenterol 2011;106:1255–1263.
31. Fraquelli M, Branchi F. The role of transient elastography in patients with hepatitis B viral disease. Dig Liver Dis 2011; 43(Suppl 1):S25–S31.
32. Hirooka M, Koizumi Y, Hiasa Y, et al. Hepatic elasticity in patients with ascites: evaluation with real-time tissue elastography. AJR Am J Roentgenol 2011;196:W766–771.
33. Huwart L, Sempoux C, Vicaut E, et al. Magnetic resonance elastography for the noninvasive staging of liver fibrosis. Gastroenterology 2008;135:32–40.
34. Luciani A, Vignaud A, Cavet M, et al. Liver cirrhosis: intravoxel incoherent motion MR imaging—pilot study. Radiology 2008;249: 891–899.
35. Annet L, Materne R, Danse E, Jamart J, Horsmans Y, Van Beers BE. Hepatic flow parameters measured with MR imaging and Doppler US: correlations with degree of cirrhosis and portal hypertension. Radiology 2003;229:409–414.
36. Tsushima Y, Blomley MJ, Kusano S, Endo K. Measuring portal venous perfusion with contrast-enhanced CT: comparison of direct and indirect methods. Acad Radiol 2002;9:276–282.
37. Tsuboyama T, Onishi H, Kim T, et al. Hepatocellular carcinoma: hepatocyte-selective enhancement at gadoxetic acid-enhanced MR imaging—correlation with expression of sinusoidal and canalicular transporters and bile accumulation. Radiology 2010;255: 824–833.
38. Colloredo G, Guido M, Sonzogni A, Leandro G. Impact of liver biopsy size on histological evaluation of chronic viral hepatitis: the smaller the sample, the milder the disease. J Hepatol 2003; 39:239–244.
39. Hopper I, Kemp, W, Porapakkham P, et al. Impact of heart failure and changes to volume status on liver stiffness: non-invasive assessment using transient elastography. Eur J Heart Fail 2012; 14:621–627.
40. Yoshida H, Shiratori Y, Moriyama M, et al. Interferon therapy reduces the risk for hepatocellular carcinoma: national surveillance program of cirrhotic and noncirrhotic patients with chronic hepatitis C in Japan. IHIT Study Group. Inhibition of Hepatocarcinogenesis by Interferon Therapy. Ann Intern Med 1999;131: 174–181.

VOLUME 31 · NUMBER 6 · FEBRUARY 20 2013

JOURNAL OF CLINICAL ONCOLOGY

ORIGINAL REPORT

Low Hepatitis C Viral Load Predicts Better Long-Term Outcomes in Patients Undergoing Resection of Hepatocellular Carcinoma Irrespective of Serologic Eradication of Hepatitis C Virus

Junichi Shindoh, Kiyoshi Hasegawa, Yutaka Matsuyama, Yosuke Inoue, Takeaki Ishizawa, Taku Aoki, Yoshihiro Sakamoto, Yasuhiko Sugawara, Masatoshi Makuuchi, and Norihiro Kokudo

Junichi Shindoh, Kiyoshi Hasegawa, Yutaka Matsuyama, Yosuke Inoue, Takeaki Ishizawa, Taku Aoki, Yoshihiro Sakamoto, Yasuhiko Sugawara, and Norihiro Kokudo, University of Tokyo; Masatoshi Makuuchi, Japan Red Cross Medical Center, Tokyo, Japan.

Published online ahead of print at www.jco.org on November 5, 2012.

Supported by Health and Labor Sciences Research Grant No. H21-015 for Clinical Cancer Research and by a grant from the Japanese Foundation for Multidisciplinary Treatment of Cancer.

Authors' disclosures of potential conflicts of interest and author contributions are found at the end of this article.

Corresponding author: Junichi Shindoh, MD, PhD, Hepato-Biliary-Pancreatic Surgery Division, Department of Surgery, Graduate School of Medicine, University of Tokyo, 7-3-1 Hongo, Bunkyo-ku, Tokyo, 113-8655 Japan; e-mail: shindou-tky@umin.ac.jp.

0732-183X/13/3106-766/$20.00

DOI: 10.1200/JCO.2012.44.3234

ABSTRACT

Purpose
Hepatitis C virus (HCV) infection has been recognized as a potent risk factor for the postoperative recurrence of hepatocellular carcinoma (HCC). However, little is known about the impact of HCV viral load on surgical outcomes. The study objective was to investigate clinical significance of HCV viral load on long-term outcomes of HCC.

Patients and Methods
Three hundred seventy patients who were classified as Child-Pugh class A and underwent curative liver resections for HCV-related HCC were divided into low and high viral load groups (≤ or > 5.3 $\log_{10}$IU/mL) based on the results of a minimum *P* value approach to predict moderate to severe activity of hepatitis; the clinical outcomes were then compared.

Results
The 5-year recurrence-free survival rate was 36.1% in the low viral load group and 12.4% in the high viral load group ($P < .001$). The 5-year overall survival rate was 76.6% in the low viral load group and 57.7% in the high viral load group ($P < .001$). Multivariate analysis confirmed significant correlation between high viral load and tumor recurrence with a hazard ratio of 1.87 (95% CI, 1.41 to 2.48; $P < .001$). Subanalysis revealed that the favorable results in the low viral load group were not attributed to whether or not serologic eradication of HCV was obtained both in primary and recurrent lesions.

Conclusion
Low HCV viral load predicts better long-term surgical outcomes in patients with HCC regardless of the serologic eradication of HCV.

J Clin Oncol 31:766-773. © 2012 by American Society of Clinical Oncology

INTRODUCTION

Recent developments in medical and surgical treatments have significantly improved the long-term outcomes of patients with hepatocellular carcinoma (HCC).[1] However, the cumulative recurrence rate remains as high as 50% to 60% at 3 years and 70% to 100% at 5 years, even after curative liver resection.[2-7]

Hepatitis C virus (HCV), a major cause of chronic hepatitis and liver cirrhosis, has been recognized as a potent risk factor of carcinogenesis[8] and/or the recurrence of HCC.[9,10] Because postoperative persistent viremia is thought to be the main cause of sustained liver dysfunction and the high tumor recurrence rate in patients with HCV, adjuvant antiviral therapy using interferon (IFN) has recently been attempted, and favorable outcomes have been reported in several studies.[11-13]

Conventionally, the eradication of HCV and a sustained status of undetectable HCV-RNA have been regarded as the most important factors for obtaining better clinical results after IFN therapy. In recent studies, however, possibly favorable effects of a reduced viral load on long-term outcomes have been suggested in patients with chronic hepatitis.[14,15]

Our hypothesis was that a correlation existed between the HCV viral load and long-term surgical outcomes. Simply labeling patient as having viremia did not sufficiently stratify those who had low viral load versus those who had high viral load. In this study, we tested this hypothesis by examining patients who had undergone curative

liver resection for HCV-related HCC and analyzed the impact of the HCV viral load on postoperative outcomes.

PATIENTS AND METHODS

Study Population

This study was performed in accordance with the ethical guidelines for clinical studies at the University of Tokyo Hospital (Tokyo, Japan). The subject pool consisted of 508 consecutive patients who underwent curative liver resection for HCV-related HCC between January 2002 and December 2011. Patients classified as Child-Pugh class B (n = 49) or patients missing preoperative viral load data (n = 89) were excluded because the goal of this study was to reveal the prognostic impact of the HCV viral load in patients who were considered to be capable of tolerating antiviral therapies. The remaining 370 patients were included in the analysis.

Serum HCV-RNA Quantification

Serum HCV-RNA was quantified within 4 weeks before surgery using a conventional reverse transcriptase polymerase chain reaction (PCR) assay before 2007 and a new commercially available real-time PCR assay (TaqMan PCR; Roche Molecular Systems, Pleasanton, CA) in 2007 and thereafter. In this study, the viral load unit was standardized to a logarithm style ($\log_{10}$IU/mL) for the statistical analysis according to the following equation: Y ($\log_{10}$IU/mL) = $\log_{10}$ [X (kIU/mL) $\times$ 10^3].

Surgical Treatment and Histopathologic Assessments

The indications for hepatic resection and the types of operative procedures were determined as previously described.[16] Briefly, operative decisions were based on an algorithm consisting of the presence of ascites, the serum total bilirubin level, and the results of an indocyanine green tolerance test.[17] Because HCC has a high propensity to invade the portal veins and because intrahepatic metastasis via vascular invasion is one of the major forms of recurrence, tumor-bearing portal regions (ie, the segment or subsegment of the liver) were systematically removed (ie, an anatomic resection) to reduce the risk of local recurrence as long as such resections were feasible given the functional reserve of the liver.[18]

The histologic classifications of the tumor and background liver were described based on the system of the Liver Cancer Study Group of Japan.[19] The histologic differentiation of HCC (well, moderate, or poor) was determined according to the Edmondson grade.[19,20] Both the fibrotic stage and the activity of the hepatitis in the background liver were also recorded according the classification proposed by Desmet et al.[21]

Postoperative Antiviral Therapy

Postoperative adjuvant IFN therapy was performed only in patients who had a good performance status and were capable of tolerating a standard high-dose combination therapy with ribavirin. Specifically, patients who were younger than 65 years of age, had no evidence of cirrhosis, and had a sufficient platelet count ($> 9.0 \times 10^4/\mu$L) were considered good candidates for postoperative antiviral therapy.

Patient Follow-Up

All patients were regularly screened for recurrences through the evaluation of the HCC-specific tumor markers α-fetoprotein (AFP) and des-γ-carboxyprothrombin every 1 to 2 months, with ultrasonography every 2 months, and with dynamic computed tomography every 4 months, as previously reported.[22] The HCV viral load was re-examined after surgery in possible candidates for adjuvant antiviral therapy. The function of the background liver was monitored using the serum ALT levels. If the ALT levels increased beyond 100 IU/L, an appropriate dose of ursodeoxycholic acid and/or monoammonium glycyrrhizinate was administered expecting their liver protective effects.[23,24]

Recurrence was defined as the appearance of a new lesion with radiologic features compatible with HCC, as confirmed using at least two imaging modalities. When a recurrence was detected, the patient received further treatment using a repeated hepatectomy, radiofrequency ablation, transcatheter arterial chemoembolization (TACE), or other treatment options, as indicated. In the present study, recurrence-free survival (RFS) was defined as the interval between the operation and the date of the diagnosis of the first recurrence or the last follow-up examination, and overall survival (OS) was calculated based on the time from surgery to death or last follow-up.

Data Analysis

Statistical analysis was performed using SAS software, version 9.3 (SAS Institute, Cary, NC). Medians and ranges of continuous data were compared using the Mann-Whitney U test. Categorical data were compared using Pearson's χ^2 test or Fisher's exact test as appropriate. $P < .05$ was considered statistically significant.

High viral load was defined as HCV viral load to predict moderate to severe activity of hepatitis (grade 2 or 3 in Desmet classification[21]). The cutoff value was determined using the minimum P value approach, and clinical outcomes were compared between the patients with a high viral load and those with a low viral load. In addition, the low viral load group was further subclassified according to whether or not HCV-RNA was detectable, and clinical outcomes between these subgroups were also compared.

Survival curves for OS and RFS were generated using the Kaplan-Meier method and were compared using the log-rank test. To identify risk factors for tumor recurrence, multivariate regression analysis was performed with the Cox proportional hazards model using a backward elimination procedure. To prevent overfitting, only factors that showed statistically significant association with tumor recurrence with $P < .10$ were included in the final model. Prognostic value of HCV viral load was

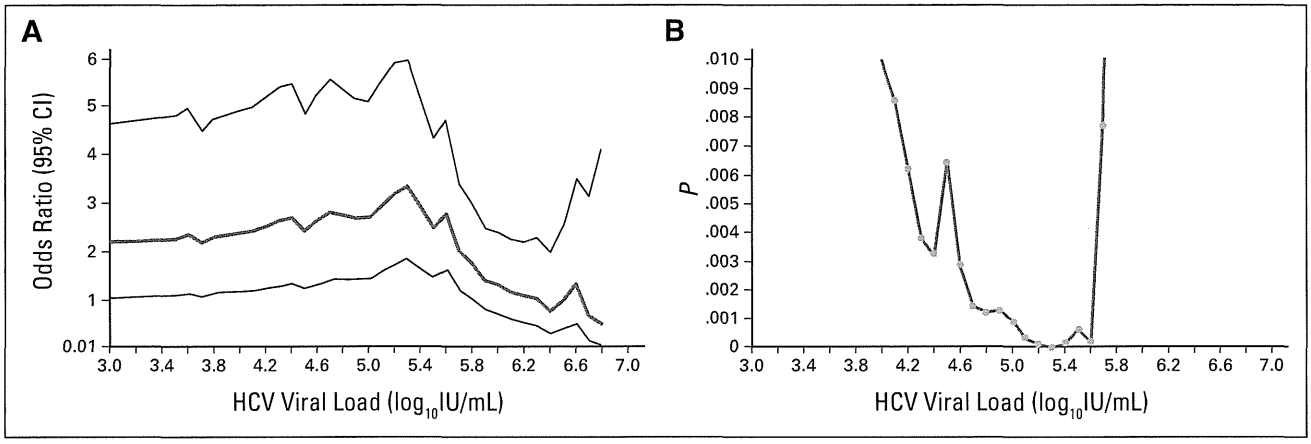

Fig 1. Optimal cutoff value of hepatitis C virus (HCV) RNA viral load to predict moderate to severe activity of hepatitis. (A) Plot of odds ratio. (B) Plot of P value in likelihood test (null hypothesis: odds ratio, 1).

Table 1. Baseline Demographics and Clinical Characteristics

Characteristic	Patients With Low Viral Load (n = 168) No.	%	Patients With High Viral Load (n = 202) No.	%	*P*
Age, years					.07
Median	69		70		
Range	47-83		39-85		
Sex					
Male	139	82.7	131	64.9	< .001
Female	29	17.3	71	35.1	
HBsAg					
Positive	7	4.2	4	2.0	.24
Negative	161	95.8	198	98.0	
HBcAb					
Positive	45	28.5	59	33.7	.30
Negative	113	71.5	116	66.3	
HCV genotype					
1b	40	69.0	87	81.3	0.07
Other	18	31.0	20	18.7	
HCV-RNA, $\log_{10}$IU/mL					< .001
Mean	3.0		6.0		
Standard deviation	1.9		0.4		
History of IFN therapy					
Positive	69	41.6	48	24.0	< .001
Negative	97	58.4	152	76.0	
No. of tumors					
Solitary	107	63.7	127	63.2	.87
Multiple	61	36.3	75	37.1	
Maximum diameter of the tumor, mm					.45
Median	24		25		
Range	8-130		6-200		
AST, IU/L					< .001
Median	34		49		
Interquartile range	24-56		36-63		
ALT, IU/L					< .001
Median	32		47		
Interquartile range	20-52		29-67		
Total bilirubin, mg/dL					.12
Median	0.7		0.7		
Interquartile range	0.5-0.9		0.6-0.9		
PT, %					.18
Median	82.9		82.9		
Interquartile range	73.1-94.9		75.6-98.3		
ICG-R15, %					< .001
Median	13.8		16.9		
Interquartile range	8.8-20.8		12.1-24.3		
Platelets, $10^4/\mu$L					.11
Median	14.4		14.0		
Interquartile range	11.4-19.0		10.1-17.1		
AFP, ng/mL					< .001
Median	9		15		
Interquartile range	4-42		7-99		
DCP, mAU/mL					.49
Median	32		35		
Interquartile range	17-177		19-146		

Abbreviations: AFP, α-fetoprotein; DCP, des-γ-carboxyprothrombin; HBcAb, hepatitis B core antibody; HBsAg, hepatitis B surface antigen; HCV, hepatitis C virus; ICG-R15, indocyanine green retention rate at 15 minutes; IFN, interferon; LC, liver cirrhosis; PT, prothrombin time.

quantified by comparing Harrell's concordance statistics of prognostic models based on the results of the multivariate analysis.

RESULTS

Characteristics of High and Low HCV Viral Load Groups

The best cutoff value of HCV viral load to predict moderate to severe activity of hepatitis was more than 5.3 $\log_{10}$IU/mL in both the plots of odds ratio and *P* value in the likelihood test (Fig 1). The background characteristics are compared between the high viral load (n = 202) and low viral load (n = 168) groups in Table 1. Female sex was more frequent in the high viral load group than in the low viral load group. The rates of coinfection with hepatitis B were not significantly different between the two groups. A history of IFN therapy was more common in the low viral load group. Number and maximum diameter of lesions were comparable between the two groups. The serum ALT and AST levels, indocyanine green retention rate at 15 minutes, and AFP levels were significantly higher in the high viral load group, whereas the platelet count was almost the same between the groups.

As for surgical factors (Table 2), the initial hepatectomy rates were 51.8% and 67.3% in the low and high viral load groups, respectively ($P < .001$). The remaining patients had repeat hepatectomies for

Table 2. Surgical, Histopathologic, and Postoperative Factors

Factor	Patients With Low Viral Load (n = 168)		Patients With High Viral Load (n = 202)		*P*
	No.	%	No.	%	
Surgical factors					
Liver resection					< .001
First HX	87	51.8	136	67.3	
≥ Second HX	81	48.2	66	32.7	
Operation time, minutes					.06
Median	359		330		
Interquartile range	279-461		263-443		
Blood loss, g					
Median	700		660		.77
Interquartile range	370-1,059		350-1,050		
Transfusion	7	4.2	7	3.5	.79
Anatomic resection	73	43.5	80	39.6	.45
Surgical margin, mm					.20
Mean	3.1		3.6		
Standard deviation	5.4		4.9		
Histopathologic factors					
Tumor differentiation*					
Well	35	21.5	42	21.2	.86
Moderate	106	65.0	134	67.7	
Poor	22	13.5	22	11.1	
Major vascular invasion	10	5.9	5	2.6	.39
Microvascular invasion	59	35.3	64	32.0	.50
Fibrosis score†					
F0-2	52	49.1	56	37.1	.06
F3-4	54	50.9	95	62.9	
Postoperative factors					
Adjuvant IFN therapy	6	3.6	7	3.5	1.00
HCV-RNA at 1 year, $\log_{10}$IU/mL‡					< .001
Mean	3.3		6.0		
Standard deviation	2.0		0.4		
ALT after surgery, IU/L					.004
Median	33		42		
Interquartile range	20-56		28-64		
AFP at 1 month, ng/mL					< .001
Median	4		7		
Interquartile range	3-7		4-13		
DCP at 1 month, mAU/mL					.08
Median	14		15		
Interquartile range	10-16		10-19		

Abbreviations: AFP, α-fetoprotein; DCP, des-γ-carboxyprothrombin; HCV, hepatitis C virus; HX, hepatectomy; IFN, interferon.
*Based on modification of the Edmondson grade.[19]
†Based on the classification by Desmet et al.[21]
‡Based on data from 31 and 28 patients with low viral load and high viral load, respectively.

recurrent lesions. Type of surgery (anatomic *v* nonanatomic), operating time, blood loss, and surgical margins were comparable between the groups. Histopathologically, no significant difference was observed in histologic grade of tumor or presence of vascular invasions. Fibrotic scores tended to be higher in the high viral load group.

Postoperative IFN therapy was performed in only six patients (3.6%) and seven patients (3.5%) in the low and high viral load groups, respectively. Because the median age of the patients in this study was 70 years and approximately 50% of the patients exhibited marked thrombocytopenia and/or cirrhotic changes in their background livers, the standard combination therapy of IFN with ribavirin was difficult to apply in most of the patients.

In 59 patients in whom postoperative viral load data were available, the HCV-RNA levels did not significantly change from baseline to 1 year after surgery (4.5 ± 2.0 $\log_{10}$IU/mL before surgery *v* 4.6 ± 1.9 $\log_{10}$IU/mL after surgery; $P = .78$). HCV-RNA viral load at 1 year and postoperative mean ALT levels were higher in the high viral load group. Postoperative AFP levels were also higher in the high viral load group even after curative resection.

Patient Survival

The median follow-up time of the studied population was 38.4 months (range, 1 to 120 months), and no hospital deaths occurred. During the study period, recurrence was observed in 108 patients (60.7%) and 137 patients (71.4%) in the low and high viral load groups, respectively.

The 1-, 3-, and 5-year RFS rates were 66.1%, 37.4%, and 36.1% in the low viral load group and 60.2%, 25.8%, and 14.9% in the high viral load group, respectively ($P < .001$; log-rank test). The 3- and 5-year OS rates were 87.6% and 76.6% in the low viral load group and 77.2% and 57.7% in the high viral load group, respectively ($P < .001$; log-rank test; Fig 2). At the time of the first recurrence, multiple intrahepatic recurrences were more frequent in the high viral load group (47.5%) than in the low viral load group (33.8%; $P = .05$). Repeat hepatectomy, radiofrequency ablation, and TACE were performed for intrahepatic recurrence in 26.0% (n = 33), 19.7% (n = 25), and 42.5% (n = 54) of patients in the high viral load group, respectively, and 41.0% (n = 34), 20.5% (n = 17), and 30.1% (n = 25) of patients in the low viral load group, respectively ($P = .06$).

The median HCV viral load of the positive HCV-RNA subgroup in the patients with low viral load was 4.9 $\log_{10}$IU/mL (range, 2.3 to 5.3 $\log_{10}$IU/mL), and it was significantly lower than that in the high viral load group ($P < .001$). Clinicopathologic parameters were almost comparable between the two subgroups in the low viral group except that HCV-RNA titers and serum AST and ALT levels were significantly higher in positive HCV-RNA patients ($P < .001$). The 1- and 3-year RFS rates were similar between the two subgroups (65.6% and 38.8% for the negative HCV-RNA patients and 66.5% and 35.9% for the positive HCV-RNA patients, respectively; $P = .61$; Fig 3A). The RFS rate among the low viral load group with positive HCV-RNA was superior to that of the high viral load group ($P = .009$). A similar tendency was also observed in the OS rates. The positive HCV-RNA patients had relatively favorable results, similar to the negative HCV-RNA patients when the viral load was ≤ 5.3 $\log_{10}$IU/mL. The 3- and 5-year OS rates were 85.8% and 78.1% for the negative HCV-RNA patients, respectively, and 89.0% and 75.8% for the positive HCV-RNA patients, respectively ($P = .94$; Fig 3B). The OS rate of the low viral load group with positive HCV-RNA was superior to that of the high viral load group ($P = .005$). These observations were constant when stratifying the study population according to hepatectomies for primary or recurrent lesions (Appendix Fig A1, online only).

Risk Factors for Postoperative Recurrence

Risk factors for postoperative recurrence were investigated in 357 patients without postoperative antiviral therapy. In the multivariate analysis, we chose 17 potential confounders considering their clinical significance and reported evidences,[4,25-31] as indicated in Table 3. There were no specific combinations of factors suggesting multicollinearity in scatter plots. In multivariate analysis, high HCV viral load (> 5.3 $\log_{10}$IU/mL), macroscopic vascular invasion, repeat resection for recurrent tumor, tumor exposure, and tumor size greater than 2 cm were selected in the final model. The concordance statistic of the four-factor model (macroscopic vascular invasion + repeat resection + tumor exposure + size > 2 cm) was 0.603 (95% CI, 0.559 to 0.647),

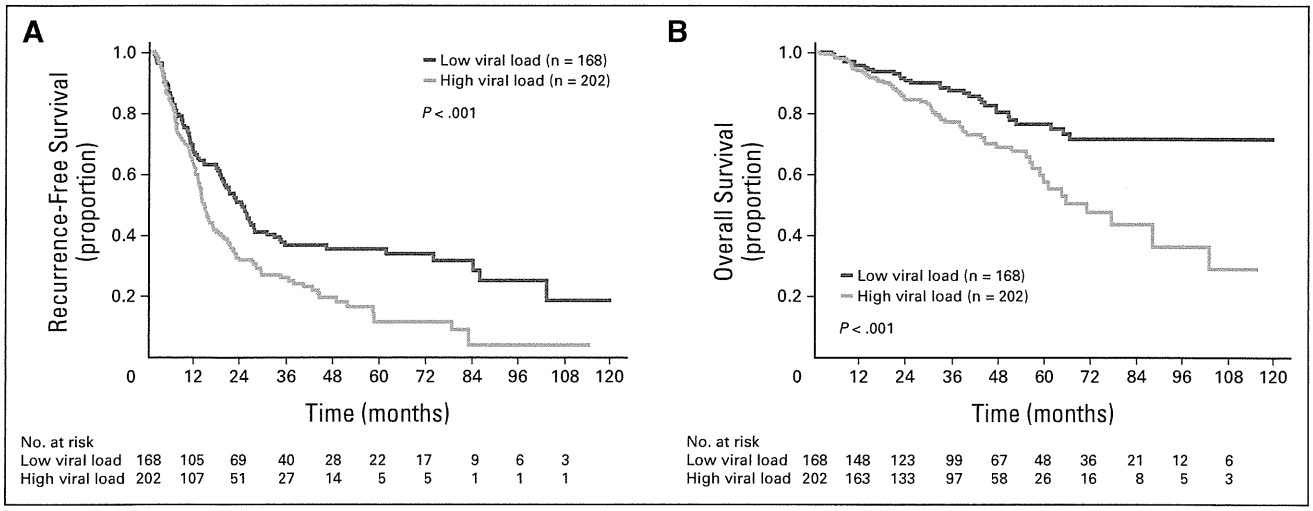

Fig 2. (A) Cumulative recurrence rate and (B) cumulative overall survival curves of low and high viral load groups.

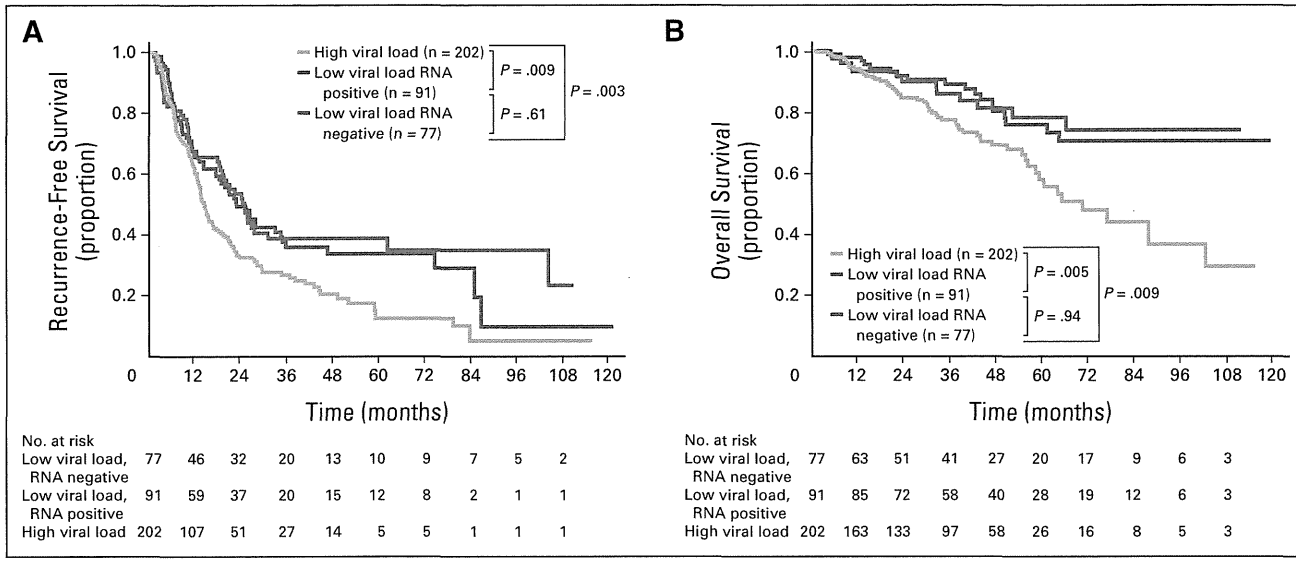

Fig 3. (A) Cumulative recurrence rate and (B) cumulative overall survival curves of low and high viral load groups stratified according to the results of hepatitis C virus RNA quantification.

and it improved to 0.627 (95% CI, 0.590 to 0.665) when including HCV viral load greater than 5.3 $\log_{10}$IU/mL in the prognostic model (Table 3).

DISCUSSION

In this study, we analyzed 370 patients who underwent curative liver resection for HCV-related HCC. The current study indicates that a low viral load ($\leq$ 5.3 $\log_{10}$IU/mL) is strongly associated with lower recurrence rate and better OS regardless of the serologic eradication of HCV. These observations were constant both in initial hepatectomy for primary lesions and repeat hepatectomy for recurrent lesions. Multivariate analysis confirms that a high HCV viral load ($>$ 5.3 $\log_{10}$IU/mL) is an independent factor associated with a 1.84-fold greater risk of tumor recurrence after curative resection of HCC.

In patients with HCV-related HCC, virologic status of HCV has been thought to be a prognostic factor associated with high tumor recurrence rate.[9,10] Adjuvant antiviral therapy is performed with the aim of preventing tumor recurrence by improving the fibrotic status and/or activity of inflammation in the background liver through the reduction of the viral load. Several studies have shown favorable long-term outcomes of adjuvant IFN therapy after locoregional treatments or surgical resections.[11,32-34] However, the effectiveness of antiviral therapy has been discussed mainly from the view point of virus eradication,[11-13,34-36] and little is known about the significance of the viral load itself for tumor recurrence.

Akamatsu et al[37] previously reviewed 371 patients who had undergone locoregional treatments for HCV-related HCC and denied a correlation between the viral load and the recurrence rate of HCC. However, their study contained a heterogeneous population that underwent

Table 3. Factors Associated With Recurrence of Hepatocellular Carcinoma

Factor	P*	Coefficient†	SE	Wald χ^2	HR	95% CI
HCV-RNA > 5.3 $\log_{10}$IU/mL	< .001	0.627	0.144	19.1	1.87	1.41 to 2.48
Macrovascular invasion	< .001	1.384	0.327	17.9	3.99	2.10 to 7.57
Repeat resection for recurrence	< .001	0.505	0.150	11.4	1.66	1.24 to 2.22
Tumor exposure	.013	0.337	0.136	6.1	1.40	1.07 to 1.83
Tumor size > 2 cm	.093	0.252	0.150	2.8	1.29	0.96 to 1.83

NOTE. The concordance statistic for the four-factor model (macrovascular invasion + repeat resection + tumor exposure + size > 2 cm) was 0.603 (95% CI, 0.559 to 0.647). The concordance statistic for the full model (the four-factor model + HCV-RNA > 5.3 $\log_{10}$IU/mL) was 0.627 (95% CI, 0.590 to 0.665). Multivariate Cox regression was applied with stepwise backward selection. Initially, all factors were included in the model. Then factors that showed no or limited statistically significant association ($P > .01$) with tumor recurrence adjusted for the remaining factors in the model were deleted from the model in a stepwise fashion. The 17 factors tested were as follows: sex, primary versus repeat resection, tumor size (> *v* ≤ 2 cm), number of tumors (solitary *v* multiple), hepatitis B core antibody (yes *v* no), HCV viral load (> *v* ≤ 5.3 $\log_{10}$IU/mL), fibrotic status of the underlying liver (F3-4 *v* F0-2), serum ALT level (> *v* ≤ 40 IU/L), indocyanine green retention rate at 15 minutes (> *v* ≤ 15%), serum α-fetoprotein level (> *v* ≤ 20 ng/mL), plasma des-γ-carboxyprothrombin level (> *v* ≤ 40 mAU/mL), type of hepatectomy (anatomic *v* nonanatomic), perioperative transfusion (yes *v* no), tumor exposure (yes *v* no), microvascular invasion (yes *v* no), macrovascular invasion (yes *v* no), and tumor differentiation (well/moderate *v* poor).

Abbreviations: HCV, hepatitis C virus; HR, hazard ratio.

*Based on likelihood test adjusted for the other factors in the final model.

†Estimated coefficient for the variable and the associated SE.

various types of treatments including surgery, ablation, and TACE. Therefore, the true clinical influence of HCV viral load on long-term outcomes of HCV-related HCC is still unclear. In the current study, we carefully reviewed patients who underwent curative surgical resections under a consistent treatment strategy in a single high-volume hepatobiliary center. Major prognostic improvements were observed both in recurrence and survival when a low viral load was obtained according to the cutoff value (5.3 $\log_{10}$IU/mL) that was determined by the minimum *P* value approach to predict moderate to severe activity of hepatitis. Comparison of clinicopathologic factors revealed that high viral load was associated with higher serum ALT and AST levels (both before and after surgery) and higher fibrotic status. These correlations are consistent with previous reports[38,39] and suggest the higher carcinogenic potential in the background liver in patients with high HCV viral load.

Another noteworthy result is that the preferable outcomes in the low viral load group are not significantly influenced by whether or not the serologic eradication of HCV is obtained. As shown in Figure 3, when the survival curves were compared between the RNA-positive and RNA-negative patients, no significant difference was observed, although both curves represented apparently better outcomes than that for the high viral load group. We also confirmed a similar tendency both in initial hepatectomy and repeat hepatectomy in a subset analysis (Appendix Figure 1, online only). These results suggest that a lower viral load might be preferable even if the serologic eradication of HCV is not obtained, supporting the outcomes of previous studies[14,15] and a recent meta-analysis[40] studying the effectiveness of IFN therapy.

Recent introduction of combination therapy consisting of pegylated IFN and ribavirin has dramatically improved the sustained viral response rate in patients with HCV.[32,33] However, the postoperative use of IFN remains a major concern because HCC usually emerges in the liver that has been damaged over the course of decades, and accordingly, patients tend to be elderly and to exhibit cirrhotic changes. Therefore, a high-dose standard combination therapy is not always applicable because of the issue of tolerability. Furthermore, even if IFN therapy is available, a sustained viral response may not always be achievable, especially in female patients or patients infected with HCV genotype 1b, both of which have been reported as factors refractory to antiviral therapy.[41-44] In fact, the median age of the current population was 70 years, and 47.8% of the patients were clinically diagnosed with cirrhosis. The proportion of women was higher in the high viral load group, and 71.4% of the patients had genotype 1b.

Given the current results, a low HCV viral load can be a new clinical end point in adjuvant therapy for HCV-related HCC. In this context, a more tolerable antiviral therapy, including low-dose IFN therapy with prolonged therapeutic duration[45,46] or possibly a combination with protease inhibitors,[47-49] may be a therapeutic option for elderly patients or patients with liver cirrhosis. Given the fact that anatomic resection of the liver was also an independent predictor of recurrence in the multivariate analysis, combination of anatomic resection and adjuvant IFN therapy may enhance the postoperative outcomes in patients with HCV-related HCC by eradicating micrometastases and reducing the carcinogenic potential in the underlying liver.

Because this study was retrospective, prospective/randomized trials are needed to confirm the true influence of the HCV viral load and the effectiveness of adjuvant antiviral therapy on postoperative outcomes. In addition, the results of the Sorafenib as Adjuvant Treatment in the Prevention of Recurrence of Hepatocellular Carcinoma (STORM) trial, if sorafenib is found to be of benefit, will impact the selection of postoperative therapy in HCC in the near future. Given the possibility of drug interactions and competing toxicity between sorafenib and antiviral agents, further investigation on the selection of adjuvant treatment is needed, especially in patients with HCV-associated HCC.

In conclusion, a low viral load may predict lower recurrence and better survival in patients undergoing hepatic resection for HCV-related HCC irrespective of the serologic eradication of HCV. Postoperative antiviral therapy with individually adjusted intensity and incorporation of direct antiviral agents may warrant prospective study to characterize safety and impact on recurrence risk in patients undergoing surgical resection for HCV-associated HCC.

AUTHORS' DISCLOSURES OF POTENTIAL CONFLICTS OF INTEREST

Although all authors completed the disclosure declaration, the following author(s) and/or an author's immediate family member(s) indicated a financial or other interest that is relevant to the subject matter under consideration in this article. Certain relationships marked with a "U" are those for which no compensation was received; those relationships marked with a "C" were compensated. For a detailed description of the disclosure categories, or for more information about ASCO's conflict of interest policy, please refer to the Author Disclosure Declaration and the Disclosures of Potential Conflicts of Interest section in Information for Contributors.
Employment or Leadership Position: None **Consultant or Advisory Role:** None **Stock Ownership:** None **Honoraria:** None **Research Funding:** Norihiro Kokudo, Bayer, Dainippon Sumitomo **Expert Testimony:** None **Other Remuneration:** None

AUTHOR CONTRIBUTIONS

Conception and design: Junichi Shindoh, Norihiro Kokudo
Collection and assembly of data: Junichi Shindoh, Kiyoshi Hasegawa, Yosuke Inoue, Takeaki Ishizawa, Taku Aoki, Yoshihiro Sakamoto, Yasuhiko Sugawara, Masatoshi Makuuchi, Norihiro Kokudo
Data analysis and interpretation: Junichi Shindoh, Kiyoshi Hasegawa, Yutaka Matsuyama, Norihiro Kokudo
Manuscript writing: All authors
Final approval of manuscript: All authors

REFERENCES

1. Rahbari NN, Mehrabi A, Mollberg NM, et al: Hepatocellular carcinoma: Current management and perspectives for the future. Ann Surg 253:453-469, 2011
2. Belghtiti J, Panis Y, Farges O, et al: Intrahepatic recurrence after resection of hepatocellular carcinoma complicating cirrhosis. Ann Surg 214: 114-117, 1991
3. Grazi GL, Ercolani G, Pierangeli F, et al: Improved results of liver resection for hepatocellular carcinoma on cirrhosis give the procedure added value. Ann Surg 234:71-78, 2001
4. Imamura H, Matsuyama Y, Miyagawa Y, et al: Prognostic significance of anatomical resection and des-gamma-carboxy prothrombin in patients with hepatocellular carcinoma. Br J Surg 86:1032-1038, 1999
5. Kakazu T, Makuuchi M, Kawasaki S, et al: Repeat hepatic resection for recurrent hepatocellular carcinoma. Hepatogastroenterology 40:337-341, 1993
6. Nakajima Y, Ko S, Kanamura T, et al: Repeat liver resection for hepatocellular carcinoma. J Am Coll Surg 192:339-344, 2001

7. Poon RT, Fan ST, Lo CM, et al: Long-term survival and pattern of recurrence after resection of small hepatocellular carcinoma in patients with preserved liver function: Implications for a strategy of salvage transplantation. Ann Surg 235:373-382, 2002

8. Tsukuma H, Hiyama T, Tanaka S, et al: Risk factors for hepatocellular carcinoma among patients with chronic liver disease. N Engl J Med 328:1797-1801, 1993

9. Kumada T, Nakano S, Takeda I, et al: Patterns of recurrence after initial treatment in patients with small hepatocellular carcinoma. Hepatology 25:87-92, 1997

10. Yamanaka N, Tanaka T, Tanaka W, et al: Correlation of hepatitis virus serologic status with clinicopathologic features in patients undergoing hepatectomy for hepatocellular carcinoma. Cancer 79:1509-1515, 1997

11. Kubo S, Nishiguchi S, Hirohashi K, et al: Randomized clinical trial of long-term outcome after resection of hepatitis C virus-related hepatocellular carcinoma by postoperative interferon therapy. Br J Surg 89:418-422, 2002

12. Miyake Y, Takaki A, Iwasaki Y, et al: Meta-analysis: Interferon-alpha prevents the recurrence after curative treatment of hepatitis C virus-related hepatocellular carcinoma. J Viral Hepat 17:287-292, 2010

13. Singal AK, Freeman DH Jr, Anand BS: Meta-analysis: Interferon improves outcomes following ablation or resection of hepatocellular carcinoma. Aliment Pharmacol Ther 32:851-858, 2010

14. Kasahara A, Hayashi N, Mochizuki K, et al: Clinical characteristics of patients with chronic hepatitis C showing biochemical remission, without hepatitis C virus eradication, as a result of interferon therapy: The Osaka Liver Disease Study Group. J Viral Hepat 7:343-351, 2000

15. Yabuuchi I, Imai Y, Kawata S, et al: Long-term responders without eradication of hepatitis C virus after interferon therapy: Characterization of clinical profiles and incidence of hepatocellular carcinoma. Liver 20:290-295, 2000

16. Hasegawa K, Kokudo N, Imamura H, et al: Prognostic impact of anatomic resection for hepatocellular carcinoma. Ann Surg 242:252-259, 2005

17. Makuuchi M, Kosuge T, Takayama T, et al: Surgery for small liver cancers. Semin Surg Oncol 9:298-304, 1993

18. Nakashima T, Kojiro M: Pathologic characteristics of hepatocellular carcinoma. Semin Liver Dis 6:259-266, 1986

19. Liver Cancer Study Group of Japan: The General Rules for the Clinical and Pathological Study of Primary Liver Cancer (ed 5). Tokyo, Japan, Kanehara, 2008

20. Edmondson HA, Steiner PE: Primary carcinoma of the liver: A study of 100 cases among 48,900 necropsies. Cancer 7:462-503, 1954

21. Desmet VJ, Gerber M, Hoofnagle JH, et al: Classification of chronic hepatitis: Diagnosis, grading and staging. Hepatology 19:1513-1520, 1994

22. Takayama T, Makuuchi M, Hirohashi S, et al: Early hepatocellular carcinoma as an entity with a high rate of surgical cure. Hepatology 28:1241-1246, 1998

23. Combes B, Carithers RL Jr, Maddrey WC, et al: Biliary bile acids in primary biliary cirrhosis: Effect of ursodeoxycholic acid. Hepatology 29:1649-1654, 1999

24. Yamamura Y, Kotaki H, Tanaka N, et al: The pharmacokinetics of glycyrrhizin and its restorative effect on hepatic function in patients with chronic hepatitis and in chronically carbon-tetrachloride-intoxicated rats. Biopharm Drug Dispos 18:717-725, 1997

25. Fan ST, Ng IO, Poon RT, et al: Hepatectomy for hepatocellular carcinoma: The surgeon's role in long-term survival. Arch Surg 134:1124-1130, 1999

26. Vauthey JN, Lauwers GY, Esnaola NF, et al: Simplified staging for hepatocellular carcinoma. J Clin Oncol 20:1527-1536, 2002

27. Ikeda K, Marusawa H, Osaki Y, et al: Antibody to hepatitis B core antigen and risk for hepatitis C-related hepatocellular carcinoma: A prospective study. Ann Intern Med 146:649-656, 2007

28. Fuster J, García-Valdecasas JC, Grande L, et al: Hepatocellular carcinoma and cirrhosis: Results of surgical treatment in a European series. Ann Surg 223:297-302, 1996

29. Lee CS, Sheu JC, Wang M, et al: Long-term outcome after surgery for asymptomatic small hepatocellular carcinoma. Br J Surg 83:330-333, 1996

30. Yamamoto J, Kosuge T, Takayama T, et al: Recurrence of hepatocellular carcinoma after surgery. Br J Surg 83:1219-1222, 1996

31. Yamanaka N, Okamoto E, Toyosaka A, et al: Prognostic factors after hepatectomy for hepatocellular carcinomas: A univariate and multivariate analysis. Cancer 65:1104-1110, 1990

32. Ikeda K, Arase Y, Saitoh S, et al: Interferon beta prevents recurrence of hepatocellular carcinoma after complete resection or ablation of the primary tumor: A prospective randomized study of hepatitis C virus-related liver cancer. Hepatology 32:228-232, 2000

33. Shiratori Y, Shiina S, Teratani T, et al: Interferon therapy after tumor ablation improves prognosis in patients with hepatocellular carcinoma associated with hepatitis C virus. Ann Intern Med 138:299-306, 2003

34. Suou T, Mitsuda A, Koda M, et al: Interferon alpha inhibits intrahepatic recurrence in hepatocellular carcinoma with chronic hepatitis C: A pilot study. Hepatol Res 20:301-311, 2001

35. Uenishi T, Kubo S, Hirohashi K, et al: Relationship between response to previous interferon therapy and postoperative recurrence of hepatitis C virus-related hepatocellular carcinoma. Hepatol Res 24:404-412, 2002

36. Uenishi T, Nishiguchi S, Tamori A, et al: Influence of interferon therapy on outcome after surgery for hepatitis C virus-related hepatocellular carcinoma. Hepatol Res 36:195-200, 2006

37. Akamatsu M, Yoshida H, Shiina S, et al: Neither hepatitis C virus genotype nor virus load affects survival of patients with hepatocellular carcinoma. Eur J Gastroenterol Hepatol 16:459-466, 2004

38. Uenishi T, Nishiguchi S, Tanaka S, et al: Response to interferon therapy affects risk factors for postoperative recurrence of hepatitis C virus-related hepatocellular carcinoma. J Surg Oncol 98:358-362, 2008

39. Kubo S, Hirohashi K, Tanaka H, et al: Risk factors for recurrence after resection of hepatitis C virus-related hepatocellular carcinoma. World J Surg 24:1559-1565, 2000

40. Miao RY, Zhao HT, Yang HY, et al: Postoperative adjuvant antiviral therapy for hepatitis B/C virus-related hepatocellular carcinoma: A meta-analysis. World J Gastroenterol 16:2931-2942, 2010

41. Kogure T, Ueno Y, Fukushima K, et al: Pegylated interferon plus ribavirin for genotype Ib chronic hepatitis C in Japan. World J Gastroenterol 14:7225-7230, 2008

42. Sezaki H, Suzuki F, Kawamura Y, et al: Poor response to pegylated interferon and ribavirin in older women infected with hepatitis C virus of genotype 1b in high viral loads. Dig Dis Sci 54:1317-1324, 2009

43. Hadziyannis SJ, Sette H Jr, Morgan TR, et al: Peginterferon-alpha2a and ribavirin combination therapy in chronic hepatitis C: A randomized study of treatment duration and ribavirin dose. Ann Intern Med 140:346-355, 2004

44. Tsubota A, Chayama K, Ikeda K, et al: Factors predictive of response to interferon-alpha therapy in hepatitis C virus infection. Hepatology 19:1088-1094, 1994

45. Kudo M, Sakaguchi Y, Chung H, et al: Long-term interferon maintenance therapy improves survival in patients with HCV-related hepatocellular carcinoma after curative radiofrequency ablation: A matched case-control study. Oncology 72:132-138, 2007 (suppl 1)

46. Shimomura S, Ikeda N, Saito M, et al: Long-term interferon therapy after radiofrequency ablation is effective in treating patients with HCV-associated hepatocellular carcinoma. Hepatol Int 5:559-566, 2010

47. Hayashi N, Okanoue T, Tsubouchi H, et al: Efficacy and safety of telaprevir, a new protease inhibitor, for difficult-to-treat patients with genotype 1 chronic hepatitis C. J Viral Hepat 19:e134-e142, 2012

48. Poordad F, McCone J Jr, Bacon BR, et al: Boceprevir for untreated chronic HCV genotype 1 infection. N Engl J Med 364:1195-1206, 2011

49. Zeuzem S, Andreone P, Pol S, et al: Telaprevir for retreatment of HCV infection. N Engl J Med 364:2417-2428, 2011

J Gastroenterol (2013) 48:269–276
DOI 10.1007/s00535-012-0632-x

ORIGINAL ARTICLE—LIVER, PANCREAS, AND BILIARY TRACT

The efficacy of nocturnal administration of branched-chain amino acid granules to improve quality of life in patients with cirrhosis

Hisashi Hidaka · Takahide Nakazawa · Shinji Kutsukake · Yoshiki Yamazaki · Izumi Aoki · Shiro Nakano · Noriyuki Asaba · Tsutomu Minamino · Juichi Takada · Yoshiaki Tanaka · Yusuke Okuwaki · Masaaki Watanabe · Akitaka Shibuya · Wasaburo Koizumi

Received: 3 May 2012 / Accepted: 11 June 2012 / Published online: 24 July 2012

Abstract
Background Nocturnal administration of branched-chain amino acid (BCAA) granules improves serum albumin levels in patients with cirrhosis. However, it is unclear whether or not this administration method can improve the patients' quality of life (QOL). In this study, we aimed to investigate the efficacy of BCAA granules, given nocturnally, in improving QOL in these patients.
Methods We performed a multicenter, randomized controlled trial examining the comparative effects of BCAA granules given orally for 3 months with daytime or nocturnal administration in patients with compensated cirrhosis. Health-related QOL was measured by a Japanese version of the questionnaire on subjective and objective symptoms, and the Short Form-8 (SF-8) questionnaire.
Results Twenty-one patients received BCAA granules three times a day (one sachet after each meal: the daytime group), and 16 patients received the granules twice a day (one sachet after breakfast, and two sachets before bedtime: the nocturnal group). Baseline characteristics did not differ between the groups (whole cohort: Child-Pugh grade A/B, 21/16; mean age, 68.2 years). There was no significant difference in any of the subjects revealed by the questionnaire regarding subjective or objective symptoms, or by the SF-8 between the daytime group and the nocturnal group after 3 months of treatment. The daytime group showed a significant effect on general health, vitality, social functioning, mental health, and role emotional as revealed on the SF-8. Conversely, the nocturnal group exhibited a significant decrease in the occurrence of muscle cramps in the legs ($P = 0.014$) and significantly improved Fisher's ratio after 3 months ($P = 0.04$).
Conclusions Nocturnal administration of BCAA granules in patients with cirrhosis reduced the occurrence of muscle cramps in the leg but did not improve the patients' QOL.

Keywords Liver cirrhosis · Branched-chain amino acid · Quality of life

Abbreviations

AAA	Aromatic amino acid
BCAA	Branched-chain amino acid
CT	Computed tomography
HCC	Hepatocellular carcinoma
LES	Late evening snack
OGTT	Oral glucose tolerance test
PEM	Protein-energy malnutrition

The trial described in this work has been registered under the following trial number: UMIN 000005274.

H. Hidaka (✉) · T. Nakazawa · T. Minamino · J. Takada · Y. Tanaka · Y. Okuwaki · M. Watanabe · A. Shibuya · W. Koizumi
Department of Gastroenterology,
Kitasato University School of Medicine,
2-1-1 Asamizodai, Minami, Sagamihara,
Kanagawa 252-0380, Japan
e-mail: hisashi7@kitasato-u.ac.jp

S. Kutsukake
Kutsukake Clinic, Sagamihara, Japan

Y. Yamazaki
Hiratsuka Kyosai Hospital, Hiratsuka, Japan

I. Aoki
Toshiba Rinkan Hospital, Sagamihara, Japan

S. Nakano
Kakunaka Clinic, Sagamihara, Japan

N. Asaba
ASABA Clinic, Sagamihara, Japan

QOL Quality of life
SF-8 Short Form-8

Introduction

It has been reported that nutritional state influences survival in patients with liver cirrhosis [1]. The energy balance in patients with liver cirrhosis is characterized as protein-energy malnutrition (PEM), disorder of glycolysis, decline of glycogenosis, negative nitrogen balance, and hyperlipolysis [2–4]. Patients with advanced liver cirrhosis show a characteristic decrease in the plasma concentration of branched-chain amino acids (BCAAs) and an increase in aromatic amino acids (AAAs). Two large randomized trials have shown that the long-term administration of BCAA supplements decreased the progression of hepatic failure and was associated with improved survival in patients with cirrhosis [5, 6]. Moreover, nocturnal energy supplementation improved nitrogen balance and abnormal fuel metabolism in patients with cirrhosis [7–9]. As an intervention for energy malnutrition, frequent meals or a late evening snack (LES) have been recommended [7–11]. The group of Sakaida et al. (Okamototo et al. [12], Sakaida et al. [13], and Tsuchiya et al. [14]) showed that 1-week administration of a BCAA-enriched nutrient, Aminoleban EN® (Otsuka Pharmaceutical Co. Ltd., Tokyo, Japan) (210 kcal) in hospitalized patients with liver cirrhosis improved energy malnutrition, but glucose intolerance occurred 12–14. Of note, long-term use of LES for 3 months showed worsened glucose tolerance, as assessed with the 75- oral glucose tolerance test (OGTT) [15]. Fukushima et al. [16] revealed in their study that nocturnal administration of BCAA granules, giving one sachet (L-isoleucine 952 mg, L-leucine 1904 mg, L-valine 1144 mg) after breakfast and two sachets before bedtime, improved the serum albumin level in cirrhotic patients who had shown no improvement in serum albumin level with daytime BCAA administration (given with each meal). However, it is unclear whether the method of BCAA administration can improve quality of life (QOL) in patients with cirrhosis. The objective of this study was to investigate the efficacy of nocturnal administration of BCAA granules in improving QOL in patients with cirrhosis.

Patients and methods

Study design and selection of patients

Between October 2008 and September 2010, this randomized controlled study was conducted in 9 hospitals and 4 medical clinics in Japan. The protocol was undertaken with the approval of the Institutional Review Board of each participating institution and in accordance with the World Medical Association's Declaration of Helsinki (1989). The final protocol was approved by the Ethics Committee of the Kitasato University, Sagamihara, Japan (C-Ethics Committee, ID 08-438). Written informed consent was obtained from each enrolled subject. The trial described in this work has been registered under the following trial number: http://www.umin.ac.jp/ctr/index.htm, UMIN 000005274.

The inclusion criteria were patients with cirrhosis who were aged between 20 and 80 years whose serum albumin level ranged from 3.1 to 3.5 g/dl. Cirrhosis was diagnosed on the basis of clinical, radiological, and laboratory parameters, and/or liver biopsy. The patients underwent endoscopy and computed tomography (CT). Exclusion criteria were: (1) Child-Pugh score $\geq$10; (2) hepatocellular carcinoma (HCC); (3) endoscopically confirmed existing moderate or large varices and post-ligated ulcers 1 month after final esophageal variceal ligation; (4) ongoing pharmacological therapy for portal hypertension with nonselective beta-blockers, nitrates, and angiotensin II type 1 receptor blockers; (5) portal thrombosis; (6) drinking alcohol within 3 months before the start of the study; (7) a history of BCAA supplementation in the previous 3 months; (8) pregnancy; and (9) allergy or past adverse reaction to BCAA.

Instruments for QOL assessment

A disease-specific health-related quality of life (HRQOL) analysis and a cross-sectional analysis of general HRQOL were conducted using the Japanese version of questionnaires on subjective and objective symptoms in patients with liver cirrhosis, and using the Japanese version of the Medical Outcomes Study 8-Item Short-Form Health Survey (SF-8). The validity and reliability of the Japanese versions of both questionnaires have already been confirmed, as described previously [17]. The Japanese version of the questionnaires on subjective and objective symptoms comprises 6 subscales (sluggishness, fatigue, general itching, anorexia, abdominal fullness, and muscle cramps). The SF-8 comprises 8 subscales (GH, general health; PF, physical functioning; RP, role limitation due to physical problems; BP, body pain; VT, vitality; SF, social functioning; MH, mental health; RE, role limitation due to emotional problems), and all of these categories are compatible with those in the SF-8. In the present study, the score of each of the 8 subscales, the physical health component summary score (PCS), and the mental health component summary score (MCS) were measured using the norm-based scoring method, which was based on a large-scale population study conducted in Japan [17]. QOL

scores are shown as mean scores with a 95 % confidence interval (95 % CI), with the higher scores representing better QOL. In order to enhance the potential for unbiased and truthful answers, participants responded anonymously to all questions and returned the questionnaires using return stamped-addressed envelopes.

Intervention protocol

Baseline evaluation included physical examination and routine laboratory tests. Daily food intake was estimated by a self-administered questionnaire. Screening information of possibly eligible patients was transmitted to the registration center. After confirmation of eligibility, the patients were randomly assigned in a 1:1 ratio by the center to either daytime BCAA granule administration [4 g BCAA (Livact® Granules; Ajinomoto Pharmaceutical, Tokyo, Japan): L-isoleucine 952 mg, L-leucine 1904 mg, L-valine 1144 mg] after each meal, or nocturnal BCAA granule administration (4 g after breakfast and 8 g before bedtime) for 3 months. Study randomization was conducted by computer to achieve a balance between the two groups without stratification. Daily food intake was mandated by the patients' physicians in charge at 30 kcal/kg/day and 1.2 g protein/kg/day. We assessed compliance with treatment at each outpatient visit by interview.

Follow up

The initial clinical visit was 2 weeks after the introduction of treatment in both arms, with a clinical visit again after another 2 weeks. The follow-up interval was every 4 weeks. Biochemical (serum albumin, aspartate aminotransferase [AST], alanine aminotransferase [ALT], total bilirubin, free fatty acid, cholinesterase, NH3, glycated albumin, and Fisher's ratio) and hematological profiles (platelets and prothrombin time) were obtained at each consultation after the patients had had an overnight fast. After 3 months of treatment, a clinical examination was performed, and patients underwent CT examinations as part of the HCC surveillance. Adverse events arising from BCAA granule administration were defined according to the Common Terminology Criteria for Adverse Events version 3.0 or 4.0. After recruitment of the last patient, follow up was designed to be continued in both treatment arms for 3 months.

Sample size calculation and statistical analysis

To our knowledge, only one study in the literature has investigated the effect of nocturnal BCAA granule administration in patients with cirrhosis [16]. In that study, nocturnal BCAA administration improved protein metabolism, but its effect on QOL was not examined [16]. Therefore, in the present study, we calculated the sample size by estimating improvement in the serum albumin level. We estimated that the rate of improvement after 3 months of treatment would be not <50 % in the nocturnal group and at least 10 % in the daytime group. At least a 10 % failure rate in both groups was estimated previously. On the basis of a 40 % difference in the improvement rate after 3 months of follow up, a sample size of 10 patients per group would provide 80 % power with a 2-sided alpha of 0.05 by log-rank test.

Values for continuous variables are presented as means ± standard deviation (SD) or medians (ranges). The paired or non-paired Student's *t*-test was used to assess the significance of differences in the comparison of normally distributed data, and the Mann–Whitney *U*-test or the Wilcoxon test was used for the non-normally distributed data, while numerical variables were assessed by Pearson's χ^2test or Fisher's exact test, as appropriate. *P* values of <0.05 were considered to indicate statistical significance. All reported *P* values were two-sided. Analyses were performed using SPSS version 17.0 software (SPSS, Chicago, IL, USA).

Results

Between September 2008 and August 2010, total of 50 patients with liver cirrhosis were refferred for possible randomization after screening from 4 hospitals and 2 clinics of the 13 centers open to the study (Fig. 1). In all, 10 patients were excluded from randomization: 7 patients who had previously received BCAA administration, and 3 patients who were confirmed to have HCC. Forty patients were initially enrolled and randomized. However, after randomization, 3 patients in the nocturnal group opted for other treatments because their regular pharmacy could not keep up our treatment schedule with nocturnal BCAA granule administration. Therefore, 21 patients received BCAA granules three times a day (one sachet after each meal: the daytime group), and 16 patients received the BCAA granules twice a day (one sachet after breakfast and two sachets before bedtime: the nocturnal group). The contributions from the six centers were as follows: Kitasato University East Hospital, $n = 23$; Kitasato University Hospital, $n = 2$; Kutsukake Clinic, $n = 7$; Hiratsuka Kyosai Hospital, $n = 3$; Toshiba Rinkan Hospital, $n = 1$; Kakunaka Clinic, $n = 1$.

Baseline characteristics did not differ between the groups. The main characteristics of the patients are summarized in Table 1. There were no significant differences between patients randomized to the daytime group and those in the nocturnal group in any of the parameters.